

NEURODEGENERATIVE DISEASES

MEF2 is a key regulator of cognitive potential and confers resilience to neurodegeneration

Scarlett J. Barker^{1,2†}, Ravikiran M. Raju^{1,3†}, Noah E.P. Milman¹, Jun Wang¹, Jose Davila-Velderrain⁴, Fatima Gunter-Rahman¹, Cameron C. Parro¹, P. Lorenzo Bozzelli¹, Fatema Abdurrob¹, Karim Abdelaal¹, David A. Bennett⁵, Manolis Kellis^{4,6}, Li-Huei Tsai^{1,2,6*}

Copyright © 2021
The Authors, some
rights reserved;
exclusive licensee
American Association
for the Advancement
of Science. No claim
to original U.S.
Government Works

Recent increases in human longevity have been accompanied by a rise in the incidence of dementia, highlighting the need to preserve cognitive function in an aging population. A small percentage of individuals with pathological hallmarks of neurodegenerative disease are able to maintain normal cognition. Although the molecular mechanisms that govern this neuroprotection remain unknown, individuals that exhibit cognitive resilience (CgR) represent a unique source of therapeutic insight. For both humans and animal models, living in an enriched, cognitively stimulating environment is the most effective known inducer of CgR. To understand potential drivers of this phenomenon, we began by profiling the molecular changes that arise from environmental enrichment in mice, which led to the identification of MEF2 transcription factors (TFs). We next turned to repositories of human clinical and brain transcriptomic data, where we found that the MEF2 transcriptional network was overrepresented among genes that are most predictive of end-stage cognition. Through single-nucleus RNA sequencing of cortical tissue from resilient and nonresilient individuals, we further confirmed up-regulation of MEF2C in resilient individuals to a subpopulation of excitatory neurons. Last, to determine the causal impact of MEF2 on cognition in the context of neurodegeneration, we overexpressed *Mef2a/c* in the PS19 mouse model of tauopathy and found that this was sufficient to improve cognitive flexibility and reduce hyperexcitability. Overall, our findings reveal a previously unappreciated role for MEF2 TFs in promoting CgR, highlighting their potential as biomarkers or therapeutic targets for neurodegeneration and healthy aging.

INTRODUCTION

Human life span has increased substantially—nearly a decade in the United States in the past 50 years—and strides are being made to identify modifiable targets that further enhance longevity (1). However, this extension of life span is often associated with a decrease in quality of life (2), highlighting that measures to extend life span must also address how to maintain functional capacity as we age. One of the biggest obstacles to healthy aging is the substantial burden of age-related neurodegenerative diseases, such as Alzheimer's disease (AD), which almost always result in profound cognitive impairment and decline. Here, we aim to identify molecular features that preserve cognitive function and could serve as therapeutic targets for neurodegenerative diseases to foster healthy aging.

Clinicians and scientists have long documented a robust epidemiological link between cognitive, social, and physical stimulation throughout life and subsequent reduced manifestation of neurological disease in adulthood and old age (3). As a whole, these healthy lifestyle factors, or forms of enrichment, are among the most effective strategies for enhancing cognitive function at baseline and enabling cognitive resilience (CgR) to multiple forms of brain pathology later in life. They represent the only known preventative measure against aging- and disease-related cognitive decline.

Rodent studies have further confirmed the causal role that an enriched lifestyle has in mediating CgR: Providing environmental enrichment (EE) preserves cognition in the context of genetically induced neurodegeneration (4, 5). In addition to improved cognitive performance, enrichment in rodents also reverses behavioral sensitization to cocaine (6) and reduces symptoms of anxiety and depression after exposure to chronic stress (7). The extensive positive effects of an enriched environment that manifest throughout life and in response to a variety of stressors underscore the need to understand the mechanisms through which this neuroprotection is afforded. A limited number of studies have begun to identify targets/pathways that can be harnessed to confer CgR (8), but the molecular drivers endogenously recruited to actualize the phenotypic benefits of cognitive stimulation remain unknown. Elucidation of these mechanisms could lead to previously unidentified therapeutic targets for promoting cognitive health across the life span. To advance these efforts, we (i) used a mouse model of EE to recapitulate the benefits of sustained cognitive stimulation and identify key molecular regulators and (ii) analyzed three cohorts of clinically curated brain RNA sequencing data to characterize the transcriptional underpinnings of CgR in humans. These complementary approaches led us to uncover the MEF2 (Myocyte Enhancer Factor 2) family of transcription factors (TFs) as candidate targets, and by up-regulating MEF2 TFs in a mouse model of neurodegeneration, we confirmed MEF2's critical role as central drivers of environment-induced neuroprotection.

Previous work on the MEF2 family (MEF2A to MEF2D) has examined their role in neurodevelopment, implicating various members in maintaining appropriate neural transmission and regulating synaptic density (9, 10). In addition, MEF2 transcriptional activity is induced by neuronal activity (11), highlighting the importance of this family in regulating molecular responses to neural stimulation.

¹Picower Institute for Learning and Memory, Massachusetts Institute of Technology, Cambridge, MA 02139, USA. ²Department of Brain and Cognitive Sciences, Massachusetts Institute of Technology, Cambridge, MA 02139, USA. ³Division of Newborn Medicine, Boston Children's Hospital, Harvard Medical School, Boston, MA 02115, USA. ⁴Computer Science and Artificial Intelligence Laboratory, Massachusetts Institute of Technology, Cambridge, MA 02139, USA. ⁵Rush Alzheimer's Disease Center, Rush University Medical Center, Chicago, IL 60612, USA. ⁶Broad Institute of MIT and Harvard, Cambridge, MA 02142, USA.

*Corresponding author. Email: lhtsai@mit.edu

†These authors contributed equally to this work.

Genetic variants within the *MEF2C* locus have been associated with differences in human intelligence (12), implicating this family in the expression of higher-order cognitive ability. Our findings extend the function of *MEF2* beyond its well-studied roles in neurodevelopment and activity-dependent gene regulation, by establishing it as a critical and specific mediator of cognitive health across the life span.

RESULTS

Cognitive stimulation improves cognition and results in global epigenomic changes in cortical neurons of both male and female mice

The strongest epidemiological predictors of CgR are mentally stimulating activities such as high educational attainment and cognitively demanding occupations (3). These forms of enrichment have been shown to afford neurological protection from the pathology of neurodegenerative disease. We examined clinical data from the Religious Orders Study (ROS) (13) and the Rush Memory and Aging Project (MAP) (14) cohort and found that among individuals spanning a range of dementia diagnoses and pathological burdens, there was a significant ($P < 0.0001$) positive correlation between cognitive activity and end-stage cognition (Fig. 1A and table S1). To study enriching lifestyle factors in mice, researchers have used models of EE. As in humans, enrichment in mice has been shown to enhance cognition (15) and delay the onset of neurodegeneration (5, 16). We hypothesized that the molecular effects of enrichment throughout life might underlie the neural processes that are induced and maintained in individuals who ultimately display CgR later in life.

We used a paradigm in which wild-type Swiss Webster mice were weaned into EE or standard housing (SH) cages and maintained in these conditions for 1 month before downstream analysis (Fig. 1B). EE chambers were large mouse cages containing two nesting/burrowing materials, a running wheel, and toys that were changed every 3 to 4 days for novelty and exploration. By contrast, SH control mice were housed with an equal number of littermates in smaller, standard cages containing only one nesting material and no toys or running wheel. One month of exposure to EE did not affect general locomotion or center-aversion in an open-field paradigm, and did not impact body weight (fig. S1). To validate the cognitive impact of our enrichment model, we conducted a memory test based on contextual fear conditioning and found, as anticipated, that EE mice display better associative learning compared to SH controls (Fig. 1C, left; $P < 0.01$). In addition, EE mice showed enhanced fear extinction compared to SH animals, consistent with previous research (Fig. 1C, right, unpaired *t* test comparing % freezing after two shocks and % freezing on the last day of extinction training, $P = 0.5340$ for SH and $P = 0.0341$ for EE) (17).

Previous work from our laboratory demonstrated that enrichment leads to chromatin remodeling and an increase in histone modifications associated with active transcriptional states in neural tissue (18). However, the genomic loci and functional relevance associated with this remodeling remain unknown. To unbiasedly assess the changes in global chromatin landscape that occur in the neurons of enriched mice, we performed ATAC (Assay for Transposase Accessible Chromatin) sequencing (ATAC-seq) to identify regions of the genome that become more accessible after enrichment. Epigenomic accessibility reflects functional relevance, as these loci are more likely to be transcribed or operate as regulatory sites (19). We first used an antibody

for RBFOX3 (NEUN) to sort neuronal nuclei from the dissociated frontal cortices of male mice reared in EE ($n = 6$ mice) or SH ($n = 6$ mice) conditions. To validate whether this led to the successful isolation of neurons, we assessed the overlap of our ATAC-seq peaks with a known dataset of neuron-specific histone chromatin immunoprecipitation sequencing (ChIP-seq) data (20). ATAC-seq signal intensity was substantially higher in the promoters of known neuronal genes when compared to known glial genes (fig. S2A, left). Second, ATAC-seq peaks showed appropriate overlap with locations containing active histone marks in neurons and nonoverlap with loci that had repressive histone marks (fig. S2A, right).

Differential analysis between EE and SH ATAC-seq signals revealed 199 differentially accessible regions (DARs), 71% of which were more accessible in EE mice (Fig. 1D), consistent with previous work from our laboratory showing an increase in active chromatin marks after enrichment (18) (tables S2 and S3). Principal components analysis showed modest separation of EE and SH samples based on all ATAC-seq peaks (fig. S2B). We repeated this experiment in female mice and similarly found more DARs in EE mice (67% of 675 total DARs) compared to SH controls (fig. S2, C and D, and tables S4 and S5).

To probe the functional relevance of these genomic regions, we used multiple, complementary approaches to annotate all accessible regions and DARs. First, accessible regions in neurons showed a characteristic distribution of openness in introns, intergenic regions, and promoters as is characteristic of published ATAC-seq datasets (19) (Fig. 1E and fig. S2E). Sites that were more accessible in enriched neurons showed an overrepresentation of distal intergenic regions, suggesting that distal enhancers and their associated binding proteins could be preferentially recruited in response to cognitive stimulation. Second, using ChromHMM, genome-wide chromatin states were inferred from existing ChIP-seq data of histone marks from adult mouse cortical neurons. This analysis revealed an enrichment for histone marks associated with enhancer sites among DARs (fig. S2F). Last, DARs were assessed for statistical enrichment of TF-binding motifs using the software package Homer, which identified 11 motifs that were significantly overrepresented in the DARs of both enriched female and male mice (Fig. 1F, adjusted $P < 0.05$; table S6). This list could be broadly separated into the *MEF2* family (fig. S3) and members of the activating protein-1 complex, including JUNB and FOSL2/FRA2. Only one TF from this list, *MEF2C*, has been causally implicated in AD, neurodevelopmental disorders, and general intelligence via genome-wide association studies (Fig. 1F). Consistent with genomic annotation and chromHMM modeling that demonstrated differential openness of putative intergenic, enhancer regions in enriched neurons, *MEF2* TFs have been shown to predominantly bind such regions (21).

Enrichment induces a specific transcriptional signature associated with *MEF2* activity

To determine the transcriptional consequences of altered chromatin structure after enrichment, we performed RNA sequencing (RNA-seq) from cortical neurons of both male and female mice and examined gene expression after 1 month of rearing in EE or SH conditions. Neurons were again isolated using an antibody for RBFOX3 to sort nuclei from dissociated frontal cortices. Across both sexes, nuclear RNA expression correlated highly with open regions from our ATAC-seq data, with highly expressed genes showing more transposon-accessible promoters (fig. S4A and tables S7, S8). Principal component analysis showed modest separation of the EE and SH samples based

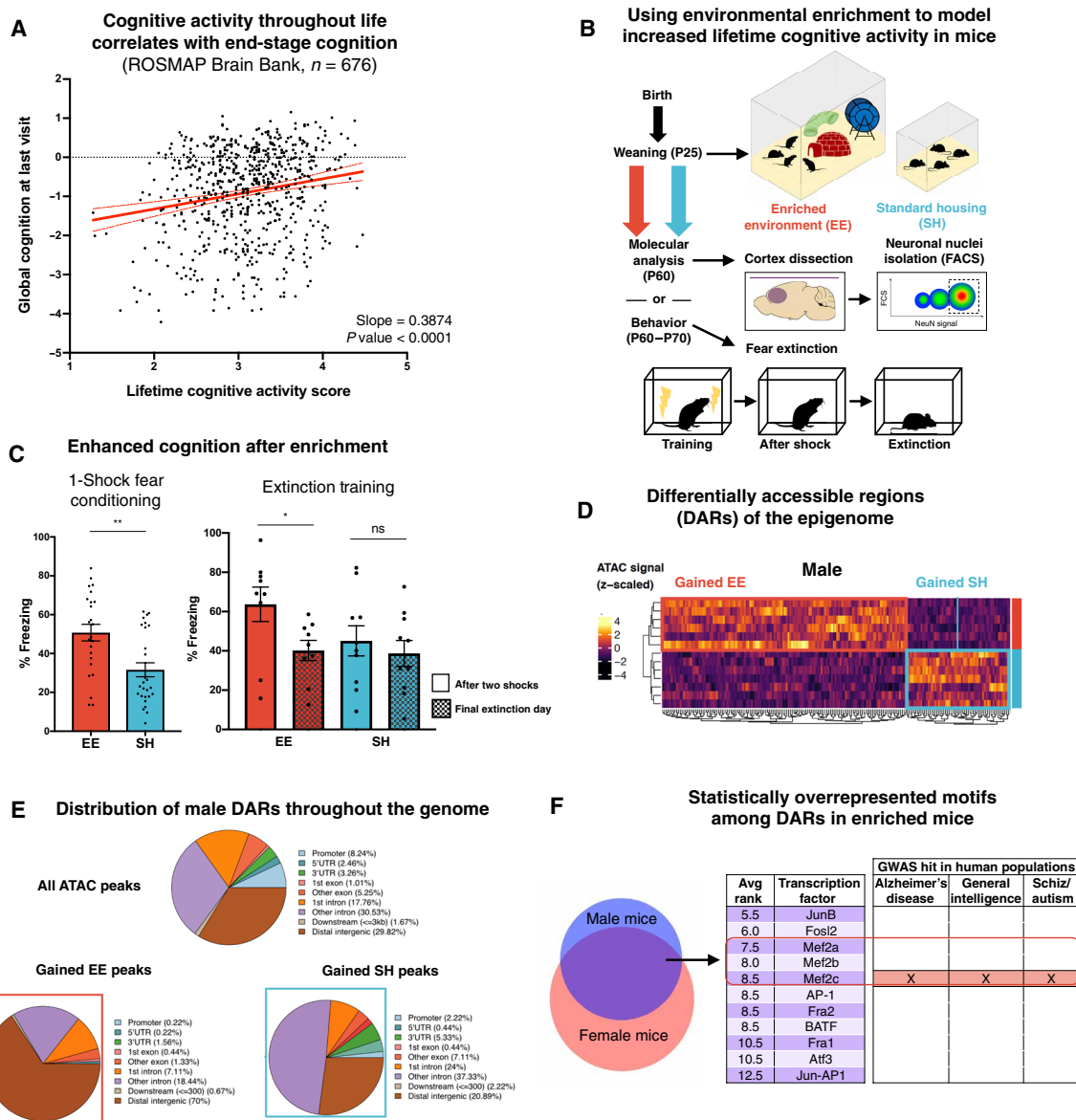


Fig. 1. Cognitive stimulation improves cognition and environmental enrichment results in global epigenomic changes in cortical neurons of mice. (A) Lifetime cognitive activity score (frequency of participation in cognitively stimulating activities) plotted against global cognitive function at last visit (an average of 19 tests) for patients in the ROSMAP cohort ($n = 676$ individuals). Solid red line represents the best fit line; dashed red lines represent 95% confidence interval. Linear regression. (B) Schematic of experimental paradigm for environmental enrichment (EE). Wild-type Swiss Webster mice were housed under standard conditions before weaning. At postnatal day 25 (P25), mice were weaned into either enriched environment (EE) or standard housing (SH) conditions. At P60, mice were subjected to molecular or behavioral analysis. (C) Left: EE and SH mice were assessed for associative learning in a contextual fear conditioning paradigm ($n = 24$ mice per group). Right: Fear extinction in EE and SH mice ($n = 10$ SH mice versus 9 EE mice). (D) Heatmap of significant ($q \leq 0.1$) differentially accessible regions (DARs) as identified via ATAC-seq of neurons isolated from the frontal cortex of EE (red, 140 DARs) and SH (blue, 59 DARs) male mice ($n = 6$ EE versus 7 SH). (E) Pie chart distribution of genomic annotations for each set of ATAC-seq peaks in males for all peaks (top), gained EE peaks (bottom left), and gained SH peaks (bottom right). 5'UTR, 5' untranslated region. (F) Left: Venn diagram of overlap between statistically overrepresented transcription factor (TF)-binding motifs among DARs in male and female EE mice. Right: List of all overlapping TFs along with their average rank (between male and female mice). Table indicating occurrence of TF in major neurocognitive-relevant GWAS (Genome-Wide Association Studies).

on all identified genes (Fig. 2A and fig. S4B). We identified 657 and 679 differentially expressed genes (DEGs) in response to enrichment [false discovery rate (FDR) < 0.1] in male and female mice, respectively (Fig. 2B, fig. S4C, and tables S10, S11). There was a statistically significant overlap of DEGs between male and female mice (53 genes, hypergeometric test, $P = 2.2 \times 10^{-11}$).

To evaluate whether the enhanced chromatin accessibility of certain TF-binding motifs after enrichment, as identified via ATAC-seq, could explain the gene expression changes observed between EE and SH neurons, we compiled lists of target genes for the top TFs whose motifs were overrepresented among regions that gained accessibility after enrichment: JUNB (22), FOSL2/FRA2 (23), MEF2A (24, 25),

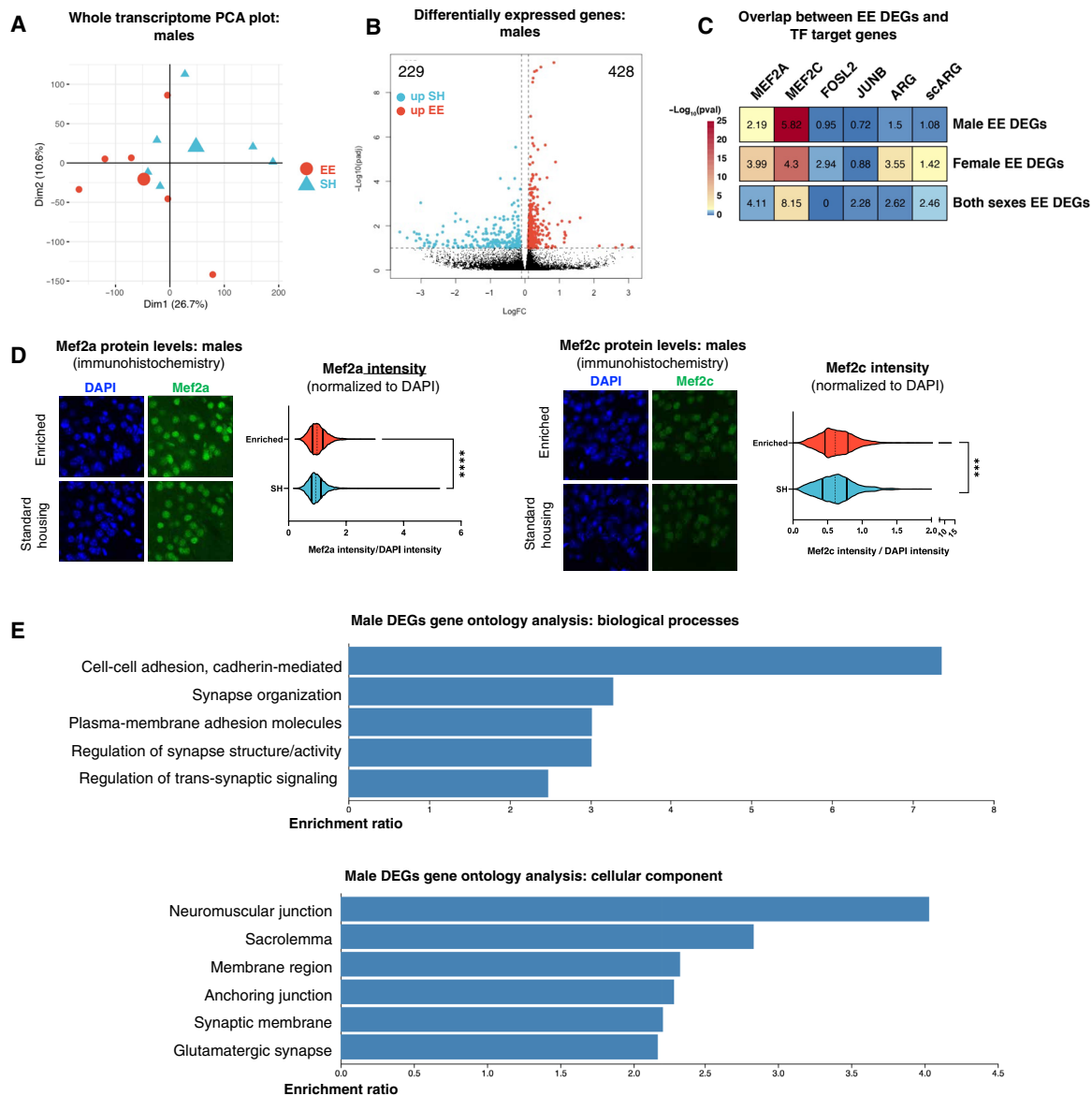


Fig. 2. Enrichment induces a transcriptional signature associated with MEF2 activity. (A) Principal component analysis (PCA) plot of nuclear RNA-seq expression data from frontal cortical neurons of EE ($n = 6$) and SH ($n = 6$) male mice. (B) Volcano plot of DEG analysis of nuclear RNA isolated from the frontal cortex of EE and SH male mice ($n = 6$ EE versus 6 SH). (C) Overlap between EE DEGs and lists of TF target genes (*Mef2a*, *Mef2c*, *Fosl2/Fra2*, and *JunB*) or activity-induced genes (*ARG* and *scARG*). Numbers in the heatmap refer to odds ratios of overlap and significance ($-\log_{10}FDR$) via hypergeometric testing denoted by color shading. (D) Left: IHC from the medial prefrontal cortex of wild-type male mice exposed to EE and SH conditions, staining for DAPI (blue), and MEF2A (green). Imaris quantification of staining with MEF2A/DAPI intensity plotted for individual nuclei across three EE and three SH wild-type mice. Right: IHC from the medial prefrontal cortex of EE and SH male mice, staining for DAPI (blue) and MEF2C (green). Imaris quantification of IHC staining with MEF2C/DAPI intensity plotted for individual nuclei across three EE and three SH mice. DAPI, 4',6-diamidino-2-phenylindole. (E) GO gene set enrichment analysis for male EE versus SH DEGs in male mice assessing for enrichment of biological processes (top) and cellular component (bottom). All terms plotted were significant at $FDR \leq 0.05$ with enrichment ratio determined as the ratio of the number of observed genes in the overlap divided by the expected number of genes given gene set sizes.

and MEF2C (25, 26). We observed the greatest degree of overlap between enrichment DEGs and target genes for MEF2C in both sexes (Fig. 2C). In addition, enrichment DEGs in female mice showed a significant degree of overlap with MEF2A targets ($P < 0.0001$). As there can be a discordance between nuclear and mature RNA expression, increases in known MEF2-regulated genes (*Zmat4*, *Astn2*, *Slc16a7*, and *Daam1*) were also confirmed via quantitative polymerase chain reaction of mature transcripts (fig. S4D) from an independent cohort of male

mice ($n = 4$ per group). Downstream targets of JUNB or FOSL2 did not show a statistically meaningful overlap with enrichment DEGs in any sex (Fig. 2C). In addition, the common DEGs present in both sexes showed specific enrichment for known MEF2C targets.

MEF2 family members exhibit activity-dependent regulation (9), and it could be hypothesized that the benefits of enrichment are simply due to increased neural activity. To assess whether up-regulation of the MEF2 network only reflects a transcriptional signature associated

with generic neuronal activity or is a specific response to sustained enrichment, we compared enrichment DEGs to two published datasets of transcriptional changes after neuronal activity. These datasets, termed scARG (single-cell Activity Related Genes) and ARG (Activity Related Genes), were generated from single-nucleus RNA sequencing of dentate gyrus neurons after brief exposure to a new environment (27) and bulk RNA sequencing after stimulating neurons in vitro and in vivo with KCl and light stimulation (28), respectively. The two lists showed a statistically significant overlap (hypergeometric test, $P = 4.2 \times 10^{-29}$), suggesting commonality in the molecular signature of immediate early gene expression after activity, independent of brain region. Enrichment DEGs in males, females, and those shared by both sexes did not show significant overlap with generic neuronal activity DEGs, with the exception of the ARG list in female mice (Fig. 2C). These results suggest that the type of neural activity arising from sustained enrichment leads to specific up-regulation of the *Mef2* transcriptional network and cannot be explained by known transcriptional networks associated with other activity-regulated TFs or generic neuronal activity alone.

Nuclear localization of MEF2 TFs is important for the activation of their transcriptional network. We assessed relative protein amounts of MEF2A and MEF2C within the nuclei of prefrontal cortex neurons after enrichment and found that MEF2A and MEF2C were significantly increased in the nuclei of both male and female mice [males in Fig. 2D, MEF2A ($P < 0.0001$) and MEF2C ($P < 0.001$); females in fig. S4E, MEF2A ($P < 0.0001$) and MEF2C ($P = 0.034$), respectively]. To determine whether the increase in nuclear MEF2 was a widespread response or limited to the prefrontal cortex, we next assessed the nuclear amounts of MEF2 in the hippocampus, another brain region critical for associative learning and affected in neurodegenerative disease. Consistent with prior reports, *Mef2c* was lowly expressed in the hippocampus, but enrichment increased nuclear MEF2A in the hippocampus of 2-month-old male and female mice exposed to 1 month of enrichment when compared to controls (males in fig. S4F, $P < 0.0001$; females in fig. S4G, MEF2A, $P < 0.0001$).

In both mice and humans, enrichment across the entire life span has been associated with cognitive benefit (29, 30). Similar to 2-month-old animals, 18-month-old wild-type C57/BL6 females demonstrated increased nuclear MEF2A and MEF2C after 1 month of enrichment, relative to SH controls (fig. S4H; $P < 0.0001$ for both MEF2A and MEF2C). Collectively, these data consistently show that the nuclear expression of MEF2 is increased upon chronic enrichment, across the life span, and in multiple brain regions in mice. To determine whether the resulting transcriptional changes are associated with known functional roles of *Mef2* TFs, we performed gene ontology (GO) analysis of enrichment DEGs. Genes that are altered in enriched male and female mice are statistically enriched for cellular components localized to dendritic spines and synapses, including ion channels and receptor complexes, and biological processes related to synapse organization/activity (Fig. 2E and fig. S5), consistent with previous work implicating various MEF2 family members in regulating synaptic density (9, 10).

Loss of *Mef2a/c* in the frontal cortex of enriched wild-type mice impairs cognitive performance and leads to neuronal hyperexcitability

Epigenomic and transcriptomic profiling, as well as immunohistochemistry, of enriched neurons suggests that MEF2 activity might play a role in mediating the phenotypic effects of EE. To determine

whether MEF2 is causally linked to the cognitive benefits of EE, we used a lentiviral construct to generate short hairpin RNA (shRNA) that would reduce the amount of endogenous MEF2A and MEF2C. Both family members were targeted because of our earlier results implicating an increase in nuclear MEF2A and MEF2C activity after enrichment, as well as previous work showing that they share a substantial proportion of chromatin binding sites (31). Control mice received a scrambled (Scrm) shRNA construct. In vitro cell culture was used to demonstrate that Scrm virus did not affect the expression of any *Mef2* members and that *Mef2a* and *Mef2c* shRNA constructs specifically knocked down their targeted TF (fig. S6A; *Mef2a*, unpaired *t* test, $P = 0.0004$; *Mef2c*, unpaired *t* test, $P = 0.0135$). Bilateral lentiviral injections into the medial frontal cortices were performed on postnatal day 30 (P30), after which mice were reared in standard cages to allow for viral shRNA expression. All mice were then moved to enrichment cages on P42 and remained in enriched environments for 30 days before downstream analysis.

Injection of MEF2 viruses led to efficient knockdown (Fig. 3A) and did not affect weight or locomotion of the animals (figs. S6, B and C). Both groups (*Mef2a/c* and Scrm) displayed equivalent initial memory acquisition, as there was no difference in the proportion of time spent freezing after receiving two foot shocks in the fear conditioning chamber. However, *Mef2a/c* knockdown in both males and females resulted in an impairment in fear extinction (males in Fig. 3B, unpaired *t* test comparing % freezing after two shocks and % freezing on the last day of extinction training, $P = 0.3047$ for *Mef2a/c* knockdown and $P = 0.0101$ for Scrm; females in fig. S6D, $P = 0.9635$ for *Mef2a/c* knockdown and $P = 0.045$ for Scrm). These results suggest that the absence of MEF2A/C impairs the molecular processes required to effectively update previously formed associations.

Studies have demonstrated that depletion of MEF2 family members has a substantial impact on electrophysiological properties of cortical excitatory neurons. Embryonic deletion of *Mef2c* in cortical excitatory neurons led to a decrease in cortical activity (26). In contrast, postnatal deletion of *Mef2c* led to increased spontaneous firing of excitatory neurons in Layers 2 and 3 of the neocortex (32). To understand the functional consequences of loss of cortical *Mef2a/c* postnatally in the context of enrichment, we performed electrophysiological recordings from pyramidal neurons harboring either *Mef2a/c* shRNA or Scrm shRNA [identified by the presence of green fluorescent protein (GFP)] after male mice were exposed to enrichment. *Mef2a/c* knockdown neurons exhibited greater membrane input resistance than control neurons (Fig. 3C, top left; unpaired *t* test, $P = 0.0010$). We observed no difference in action potential amplitude and reduced inhibitory postsynaptic current frequency (fig. S6E). The threshold of excitation was significantly reduced after *Mef2a/c* knockdown, indicating a lower threshold to fire (Fig. 3C, top right; unpaired *t* test, $P = 0.0391$). These changes in membrane properties were accompanied by a considerable increase in hyperexcitability after *Mef2a/c* knockdown [Fig. 3C, bottom; two-way analysis of variance (ANOVA), $P < 0.0001$ for group and interaction]. Other firing properties, such as action potential amplitude, were unaffected (fig. S6E). Together, these findings highlight MEF2's critical role in tempering excitatory transmission and are consistent with previous findings in which MEF2 activity was modulated postnatally (32). They are also reminiscent of early electrophysiological changes that occur in numerous neurodegenerative disorders, in which neurons show hyperexcitability in early pathological states, even before the onset of cognitive symptoms (33).

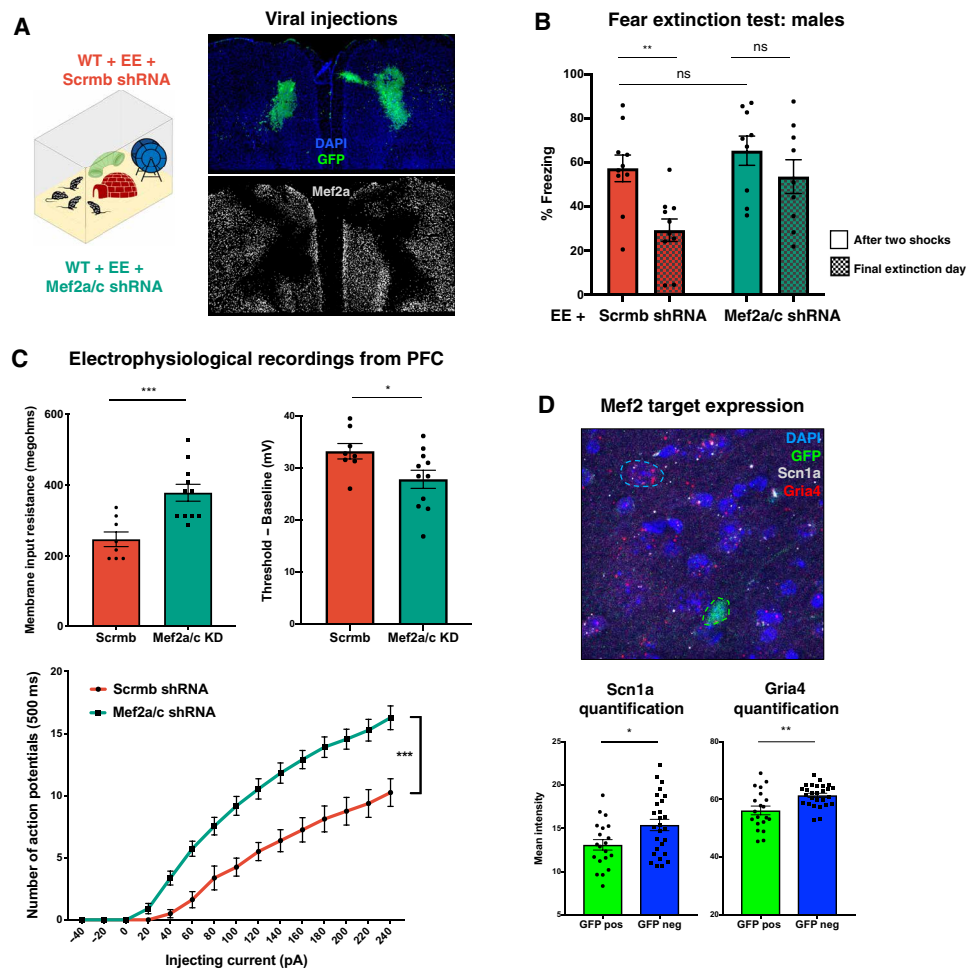


Fig. 3. Loss of *Mef2a/c* in the frontal cortex of enriched male wild-type mice impairs cognitive performance and leads to neuronal hyperexcitability. (A) Schematic of experimental paradigm for shRNA knockdown in the context of EE. On P30, wild-type (WT) Swiss Webster mice received bilateral frontal cortex injections of lentiviral vectors containing shRNA cassettes against either a scrambled sequence (Scrm, red) or *Mef2a* and *Mef2c* (*Mef2a/c*, green). shRNA cassettes also constitutively expressed GFP to aid in determining the knockdown region. Immunohistochemistry staining for DAPI (blue, top), GFP (green, top), and MEF2A (white, bottom), to show representative viral expression and *Mef2* knockdown. (B) Fear extinction testing in *Mef2a/c* shRNA-treated and Scrm-treated male mice ($n = 10$ mice per group). (C) Voltage-clamp recordings from pyramidal neurons (*Mef2a/c*, $n = 11$ cells from four animals; Scrm, $n = 8$ cells from four animals) in shRNA-expressing regions (identified by GFP fluorescence) to quantify membrane input resistance (top left), difference between baseline voltage and action potential threshold (top right), and the number of action potentials in 500 ms for a given injecting current (bottom) in both conditions. (D) Top: RNA in situ hybridization for *Scn1a* (white) and *Gria4* (red) in parallel with immunohistochemistry for GFP (green) in the frontal cortex of animals injected with *Mef2a/c* shRNA. Bottom: Quantification of *Scn1a* (left) and *Gria4* (right) intensity in either GFP positive ($n = 20$ from four animals) or GFP negative ($n = 27$ cells from four animals) cells.

Several MEF2 targets are known to regulate the resting membrane potential of neurons (34); therefore, we next examined how *Mef2a/c* knockdown in enriched animals affected downstream members of the MEF2 regulatory network. We focused on two of these genes, *Scn1a* and *Gria4*, which were also up-regulated in cortical neurons of male, enriched mice. *Scn1a* encodes part of a sodium channel and is critically involved in maintaining appropriate excitability thresholds because hundreds of mutations in this gene have been found to cause genetic epilepsy (35, 36). Similarly, *Gria4* encodes part of a glutamate-gated ion channel, and loss-of-function mutations in this gene have

also been associated with epileptic discharge (37). We used RNA in situ hybridization to measure expression of these targets in GFP-positive neurons that received shRNA against *Mef2a/c* and confirmed that *Scn1a* and *Gria4* are decreased in neurons lacking *Mef2a/c* (Fig. 3D; *Scn1a* unpaired *t* test, $P = 0.0168$; *Gria4* unpaired *t* test, $P = 0.0015$), suggesting that a MEF2-directed transcriptional program might contribute to the altered electrophysiological properties of these neurons. Collectively, these results confirm that MEF2 activity is required during enrichment to enable cognitive benefits and that blocking MEF2 activity leads to hyperexcitability in cortical neurons.

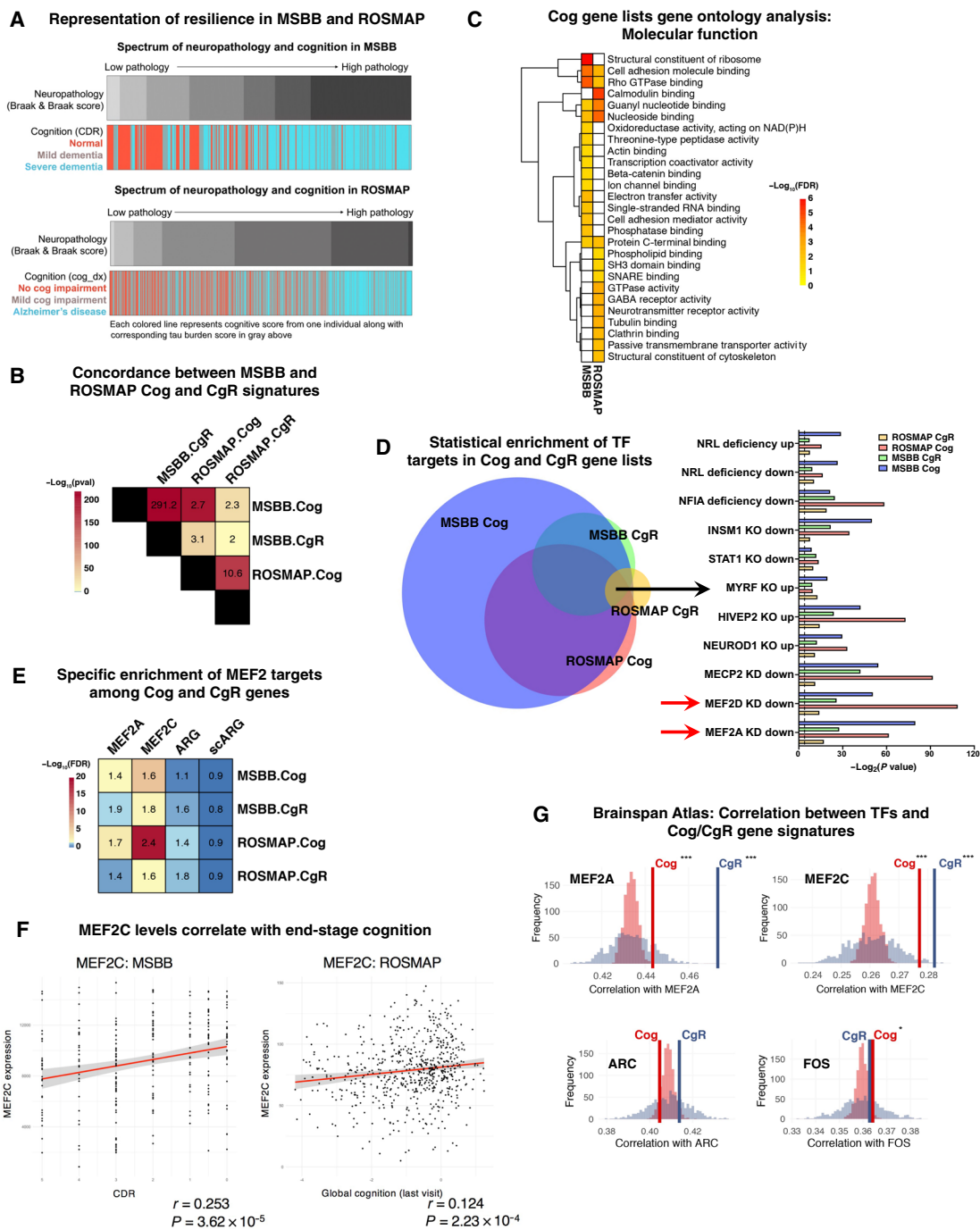
The MEF2 transcriptional network is associated with cognition and CgR in humans

To gain insight into the molecular factors that promote cognitive health and resilience in humans and assess the translational potential of MEF2-mediated cognitive benefits, we used clinical and prefrontal cortical neurotranscriptomic data from two repositories that contain both healthy control individuals and individuals suffering from AD: (i) Mount Sinai Brain Bank (MSBB), $n = 260$, and (ii) ROSMAP, $n = 636$. Although MSBB and ROSMAP contain transcriptomic data for multiple brain regions, we chose to focus on the anterior prefrontal cortex to parallel our mouse epigenomic and transcriptomic studies. In addition, the anterior prefrontal cortex is critically involved in working memory and other executive functions that deteriorate in AD (38).

As expected in both datasets, end-stage cognitive function was significantly correlated with both β -amyloid plaque density (MSBB, $P < 2 \times 10^{-16}$; ROSMAP, $P < 2 \times 10^{-16}$) and tau burden (Braak stage; MSBB, $P < 2 \times 10^{-16}$; ROSMAP, $P < 2 \times 10^{-16}$), with higher amounts of pathology predicting worse cognition

(Fig. 4A). However, a small subset (<10%) of individuals exhibited CgR, defined as the absence of dementia despite the presence of extensive amyloid and tau pathology (fig. S7A). For each dataset, we generated two lists of genes that were associated with cognitive function. The first list, termed Cog, contained genes whose expression significantly ($FDR < 0.05$) correlated with end-stage cognition in a simple linear regression. The second list, termed CgR, included genes whose expression correlated ($FDR < 0.05$) with end-stage cognition in a multiple linear regression controlling for other potential clinical predictors of cognitive decline—age at death, sex, and

Fig. 4. The MEF2 transcriptional network is associated with CgR in humans. (A) Spectrum of neuropathology and cognition in the MSBB ($n = 260$, top) and ROSMAP ($n = 636$, bottom) cohort, with each individual represented as a vertical line across the neuropathology (Braak & Braak score) and cognition bars. **(B)** Overlap analysis of cognition (Cog)– and cognitive resilience (CgR)–associated genes in MSBB and ROSMAP cohorts. Numbers in the heatmap refer to odds ratios of overlap, and significance ($-\log_{10}$ FDR) is denoted by color shading. **(C)** GO enrichment of Cog gene sets in MSBB and ROSMAP. Shading denotes the significance ($-\log_{10}$ FDR) of GO term enrichment. GTPase, guanosine triphosphatase; NA(P)DH, reduced form of nicotinamide adenine dinucleotide phosphate; GABA, γ -aminobutyric acid; SNARE, soluble *N*-ethylmaleimide-sensitive factor attachment protein receptor. **(D)** Statistical enrichment of TF targets in Cog and CgR gene lists, from Enrichr database. Venn diagram reflects all significant ($P < 0.01$) TFs identified in each list, with arrow indicating the overlap of 10 distinct TFs in all four lists. Right: Bars indicate significance ($-\log_2[P$ value]) for overlap between each list and TF targets in a hypergeometric test. Red arrows indicate highest overall enrichment for targets of MEF2. **(E)** Cog and CgR gene sets from the MSBB and ROSMAP ($n = 636$ individuals) cohorts were assayed for enrichment among four different gene sets: MEF2A targets, MEF2C targets, Activity-related genes (ARGs), and genes associated with neuronal activity determined by single cell sequencing of neurons (scARG). Numbers in the heatmap refer to odds ratios of overlap, and significance ($-\log_{10}$ FDR) is denoted by color shading. **(F)** Gene expression of *MEF2C* from the anterior prefrontal cortex in the MSBB cohort and from the dorsolateral prefrontal cortex in the ROSMAP cohort plotted against clinical dementia rating (MSBB) and global cognitive function at last visit (ROSMAP). Each individual is represented by a dot. Red line denotes regression line with standard error (gray shading). **(G)** Pearson correlation coefficient values measuring coexpression between *MEF2A* (top left) and either MSBB Cog (bold red line) or CgR (bold blue line) gene sets across developmental time from cortical samples of the BrainSpan Atlas of the Developing Human Brain. Resampling-based statistical test performed contrasting average correlation values observed (red and blue lines) with random expectation estimated by computing average *MEF2A* coexpression values across BrainSpan Atlas for 10,000 randomly selected, same-sized gene sets (Cog = red histogram, CgR = blue histogram). Asterisks denote significant results. Similar analysis was performed for *MEF2C* (top right), *ARC* (bottom left), and *FOS* (bottom right).



Downloaded from https://www.science.org at Massachusetts Institute of Technology on November 10, 2021

neuropathological data available for all patients in the dataset. For the MSBB dataset, we controlled for plaque mean, neuropathology score, and Braak stage, whereas for the ROSMAP dataset, we

controlled for severity of global AD pathology, cerebral arteriosclerosis, cerebral amyloid angiopathy, gross and microcerebral infarctions, and hippocampal sclerosis. The Cog lists (MSBB = 6544

genes; ROSMAP = 4253 genes) and CgR lists (MSBB = 553 genes; ROSMAP = 745 genes) were highly correlated across the two human cohorts, increasing confidence in their biological validity (Fig. 4B and table S12). Within each human cohort, there was a high degree of correlation between the Cog and CgR lists, indicating that many of the same genes remain correlated with end-stage cognition even when taking other, potentially confounding clinical variables into consideration (Fig. 4B). Both Cog and CgR lists were enriched for molecular functions related to signal transduction, including PDZ domain binding, Rho guanosine triphosphatase binding, and ion channel binding, consistent with the types of gene categories that are up-regulated after chronic enrichment (Fig. 4C and fig. S7B).

Our mouse work demonstrated that MEF2 TFs are drivers of the molecular processes induced upon enrichment, the most robust predictor of CgR. To unbiasedly assess the robustness of the MEF2 signal in human signatures of cognition, we first probed Cog and CgR lists for statistical enrichment of TF targets. We used the Enrichr database (39) that contains transcriptional changes after over-expression and/or knockdown of many TFs. To generate a high confidence list, we overlapped the TFs that were identified from each of the four gene lists (MSBB Cog, MSBB CgR, ROSMAP Cog, and ROSMAP CgR), yielding a final set of 10 TFs whose targets are enriched among the genes that predict end-stage cognition (Fig. 4D). Included in this list were MEF2A and MEF2D, indicating that unbiased interrogation of transcriptional predictors of cognitive function and resilience in humans also points to the MEF2 circuit as a network of genes whose expression is associated with the maintenance of cognitive function. Of note, although the Enrichr database contains targets for most TFs, including MEF2A and MEF2D, it lacks information for MEF2C. To validate the enrichment of MEF2 targets in the Cog and CgR lists, we assessed the degree of overlap between each list and the MEF2A and MEF2C targets we previously defined by overlapping ChIP-seq data and conditional mouse knockout data. MEF2C targets were significantly enriched in all lists, whereas MEF2A targets were significantly enriched in Cog gene lists only (Fig. 4E; $P < 0.01$). Transcriptional targets of generic neural activity (ARG and scARG) were not enriched in any of the Cog or CgR lists, again indicating specificity of the MEF2 network in the genes associated with cognitive function and resilience. Last, we found that expression of MEF2C itself was positively and significantly correlated with higher cognitive function in the MSBB (Fig. 4F, left; $n = 260$, $r = 0.253$, $P = 3.62 \times 10^{-5}$) and ROSMAP (Fig. 4F, right; $n = 636$, $r = 0.124$, $P = 2.23 \times 10^{-4}$) cohorts. This was also true for MEF2A (fig. S7C; $n = 636$, $r = 0.066$, $P = 0.049$) and MEF2D (fig. S7D; $n = 636$, $r = 0.140$, $P = 2.92 \times 10^{-5}$) in the ROSMAP cohort, but not the MSBB cohort (fig. S7, C to E). MEF2A appears to be more lowly expressed in the human cortex compared to MEF2C, unlike in the mouse brain, which could provide an explanation of why MEF2C appears more strongly correlated with cognition and CgR in humans (fig. S7F).

Using a separate dataset of RNA sequencing from human cortical brain tissue across development [BrainSpan Atlas of the Developing Human Brain; (40)], we determined the coexpression values, defined as the absolute value of r in a Pearson's correlational analysis, between MEF2C and all other expressed genes from 8 weeks after conception to 12 months of age postnatally. The average correlation of all genes in the MSBB Cog and CgR lists with MEF2C (P values for Cog $< 1 \times 10^{-4}$; CgR = 0.005) was significantly higher than that observed for randomly selected, similar-sized groups of genes (10,000 iterations)

in a bootstrapping analysis (Fig. 4G). This was also true for MEF2A (P values for Cog = 0.001; CgR $< 1 \times 10^{-4}$), but less so for FOS (P values for Cog = 0.04; CgR = 0.362) or ARC (P values for Cog = 0.916; CgR = 0.295), two classic markers of neuronal activity. Analysis of the ROSMAP Cog and CgR gene sets revealed similar findings (fig. S7G; P values for MEF2A Cog $< 1 \times 10^{-4}$ and CgR = 0.01; P values for MEF2C Cog $< 1 \times 10^{-4}$ and CgR $< 1 \times 10^{-4}$; P values for ARC Cog = 0.787 and CgR = 0.247; P values for FOS Cog = 0.49 and CgR $< 1 \times 10^{-4}$). Our findings suggest that MEF2 TFs are part of a specific regulatory network that is transcriptionally more active in cognitively resilient individuals.

Single-nucleus RNA sequencing of cortical tissue from a cognitively resilient AD cohort reveals that resilience-promoting MEF2 activity is specific to a unique subpopulation of excitatory neurons

To further dissect the molecular signature of CgR, we next performed single-nucleus RNA sequencing on prefrontal cortex tissue from nine resilient and nine nonresilient individuals identified from the ROSMAP brain bank. All individuals were matched for sex (all female), age, postmortem interval, and pathological variables (fig. S8A). Resilient subjects, however, remained cognitively unimpaired before death, whereas nonresilient individuals received a final diagnosis of AD. Using the 10 \times Chromium single-cell platform and applying stringent quality control metrics (see Materials and Methods), we sequenced a total of 94,552 cells across the 18 individuals. Dimensionality reduction and clustering, via Uniform Manifold Approximation and Projection (UMAP) analysis, revealed that all cells fell into six distinct transcriptional clusters (Fig. 5A). By interrogating the expression patterns of known gene markers, we determined that the six clusters corresponded to the known major cell types in the brains (Fig. 5A and fig. S8B). Within each cell-type cluster, we performed differential gene expression analysis between resilient and nonresilient cells (table S13). GO analysis revealed that DEGs in excitatory and inhibitory neurons shared similar signatures, with enrichment for molecular functions related to protein targeting and localization and regulation of translation, suggesting that a signature of resilience may be the presence of neurons that are actively engaged in protein synthesis (Fig. 5B). To determine whether MEF2 activity was driving differential gene expression, we first assessed overall expression of MEF2A and MEF2C in each of the cell types. MEF2A was virtually unexpressed across all the cell types with only minimal expression in excitatory neurons and microglia. On the other hand, MEF2C was more robustly present, predominantly in excitatory neurons, inhibitory neurons, and microglia (Fig. 5C). Neither MEF2A nor MEF2C were differentially expressed between the resilient and nonresilient cells of any major cell type (fig. S8C). Given the heterogeneity known to be present within the major cell types of the brain, we next performed subclustering analysis, focusing first on the excitatory neurons, which revealed seven distinct subclusters (Fig. 5D). By comparing the markers of each subcluster with genes enriched in unique cortical layers as defined previously (41), we observed that the excitatory neuron subclusters are defined to a certain extent by cortical layer (Fig. 5E). GO enrichment analysis of the subcluster markers also showed functional heterogeneity in the different subclusters (Fig. 5F). Differential expression analysis between resilient and nonresilient cells in each of the subclusters demonstrated that MEF2C was specifically and uniquely up-regulated in the resilient neurons from subcluster Ex2 (Fig. 5G; FDR = 2.22×10^{-57}).

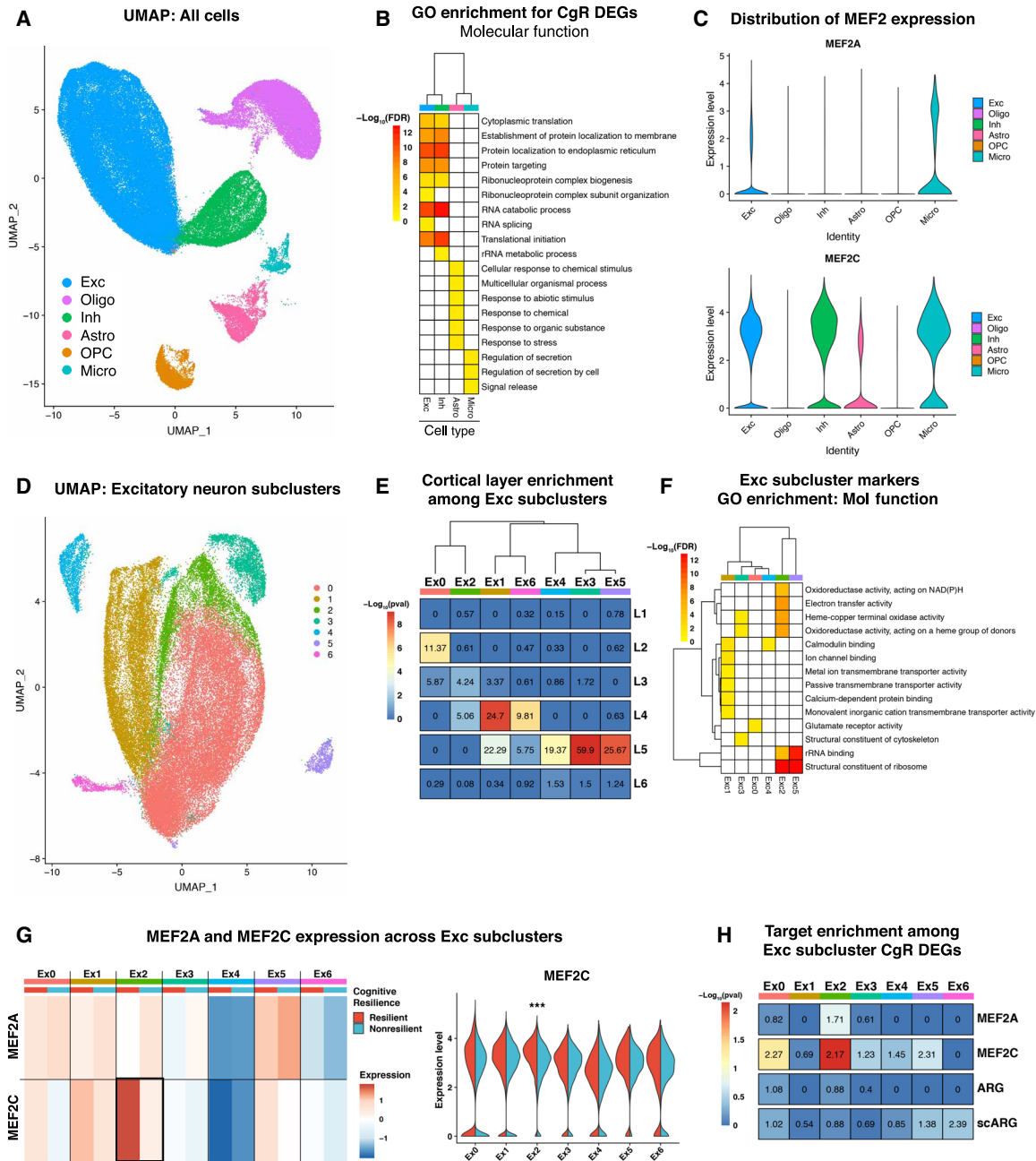


Fig. 5. Single-cell RNA sequencing of cortical tissue from a cognitively resilient cohort reveals that resilience-promoting MEF2 activity may be specific to a unique subpopulation of excitatory neurons. (A) Uniform manifold approximation and projection (UMAP) of all annotated cells ($n = 94,552$ cells from nine resilient and nine nonresilient individuals). (B) GO enrichment for molecular function terms of differentially expressed genes (DEGs) between resilient and nonresilient cells, for all cell types. Cell types not shown did not have significant GO enrichment for their DEGs. Shading denotes the significance ($-\log_{10}(\text{FDR})$) of the GO term enrichment. (C) Violin plots displaying the expression of MEF2A (top) and MEF2C (bottom) for each identified cell type cluster. (D) UMAP plot of Exc cluster from UMAP in (A) to demonstrate distinct subclusters of excitatory neurons. (E) Enrichment of Exc subcluster markers (Ex0 to Ex6) for cortical layer markers (L1 to L6) as identified previously [He *et al.* (41)]. Numbers in the heatmap are odds ratios of overlap, and significance ($-\log_{10}(\text{FDR})$) is denoted by color shading. (F) GO enrichment for molecular function terms of Exc subcluster markers. Shading denotes the significance ($-\log_{10}(\text{FDR})$) of the GO term enrichment. (G) Heatmap (left) of MEF2A and MEF2C expression in each excitatory neuron subcluster, differentiated by cells belonging to resilient (red) and nonresilient (blue) individuals. Shading denotes amount of gene expression, normalized across the row to show gene's relative expression across all subclusters. Violin plot (right) of MEF2C expression in each subcluster, divided by resilient and nonresilient cells. (H) DEGs between resilient and nonresilient cells in each of the excitatory cell subclusters were assayed for enrichment among four different gene sets: MEF2A targets, MEF2C targets, activity-related genes (ARGs), and genes associated with neuronal activity determined by single-cell sequencing of neurons (scARG). See the main text and Materials and Methods for more description of gene sets. Numbers in the heatmap are odds ratios of overlap, and significance ($-\log_{10}(\text{FDR})$) is denoted by color shading.

Ex2 showed weak enrichment for markers of L3/L4 cortical neurons, and strong enrichment for ribosomal and rRNA binding genes, suggesting that Ex2 may be a translationally active subset of neurons. Resilient DEGs in Ex2 were also enriched for known MEF2C targets (Fig. 5H). No enrichment was observed for MEF2A targets or general markers of neuronal activity (ARG and scARG lists), suggesting that the differential activity within Ex2 neurons is specific to MEF2C. Functionally, the resilient DEGs across the individual subclusters showed some commonality particularly in terms related to the structural constituent of the ribosome, electron transfer activity, and oxidoreductase activity (fig. S8D). We also performed a similar subclustering analysis on inhibitory neurons and microglia, the other MEF2C-expressing cell types, and found no differential abundance of the MEF2 TFs or enrichment of MEF2 targets in the DEGs between resilient and nonresilient cells in any of the inhibitory neuron or microglial subclusters (fig. S8, E to G). This suggests that the up-regulation of MEF2C observed in resilient cells, and the enrichment of known targets in resilient DEGs, is specific to the subpopulation of excitatory neurons in the prefrontal cortex.

Mef2a/c overexpression improves cognition and rescues tauopathy-induced hyperexcitability in a mouse model of neurodegeneration

With human bulk and single-cell transcriptomic analysis pointing to an association between neuronal *Mef2* expression and the preservation of end-stage cognition, we next asked whether enrichment and modulating MEF2 activity could promote resilience in the context of neurodegeneration. To do this, we turned to transgenic mouse models of tauopathy and neurodegeneration, which express the human tau protein harboring the P301S disease-causing mutation that leads to frontal temporal dementia (42). First, we examined published RNA sequencing data from cortical brain samples of young (3 months) and old (10 months) TAU58/2 mice and their nontransgenic littermates (43). The TAU58/2 transgenic mouse expresses the P301S tau protein under the neuronal mThy1.2 promoter. We found that the DEGs between young TAU58/2 mice and their controls were enriched for *Mef2a* and *Mef2c* targets, whereas the DEGs in the aged cohort were enriched for *Mef2c* targets (Fig. 6A). The DEGs at both ages showed no enrichment for JUNB or FOSL2 targets, or for markers of neuronal activity (ARG and scARG datasets). These data suggest that the transcriptional network induced by MEF2 activity and preserved in CgR might share salient and specific features with the one that is suppressed in P301S-induced tauopathy in both young and aged mice.

Mice harboring mutant human tau display neuronal hyperexcitability in early stages of the disease (44). We recorded from the prefrontal cortex in 4-month-old male PS19 mice exposed to either EE or SH conditions, in which the P301S protein is driven by the mouse prion protein promoter. For all PS19 experiments, only male mice were used given reports of inconsistent pathology in female mice. As anticipated, cortical neurons from PS19 mice were hyperexcitable, with significantly more action potentials fired at a constant injecting current, when compared to wild-type neurons [Fig. 6B, top; two-way ANOVA for each pairwise comparison: WT versus PS19 ($P = 0.0045$), PS19 versus PS19 + EE ($P < 0.0001$), WT versus PS19 + EE ($P = 0.0220$)]. This was accompanied by increased membrane input resistance [Fig. 6B, bottom left; independent *t* test for each pairwise comparison: WT versus PS19 ($P = 0.0050$), PS19 versus PS19 + EE ($P = 0.0036$), WT versus PS19 + EE ($P = 0.8173$)] and resting

membrane potential [Fig. 6B, bottom right; independent *t* test for each pairwise comparison: WT versus PS19 ($P = 0.0163$), PS19 versus PS19 + EE ($P < 0.0001$), WT versus PS19 + EE ($P = 0.7077$)]. Exposure to EE for 1 month completely rescued this hyperexcitability phenotype. As expected, in a PS19 background, exposure to EE increased nuclear MEF2 intensity compared to SH at both early (4 months; Fig. 6C; MEF2A, unpaired *t* test, $P < 0.0001$; MEF2C, unpaired *t* test, $P = 0.0004$) and moderate (7 months; fig. S9A; MEF2A, unpaired *t* test, $P < 0.0001$; MEF2C, unpaired *t* test, $P < 0.0001$) amounts of pathological burden. Enrichment of the older cohort of PS19 mice did not alter the amount of phosphorylated tau present (fig. S9B; P-Tau 181, unpaired *t* test, $P = 0.62$; AT8, unpaired *t* test, $P = 0.71$), as measured by two independent antibodies that detect pThr¹⁸¹ (P-Tau T181) and pSer²⁰²/pThr²⁰⁵ (AT8). This suggests that enrichment and *Mef2* induction do not substantially alter pathological progression or evolution.

If the procognitive benefits of enrichment are mediated by the transcriptional activity of MEF2, then *Mef2* overexpression in the absence of enrichment might be sufficient to enhance cognitive function and rescue hyperexcitability in P301S-induced tauopathy. Postnatal modulation of *Mef2* expression has been shown to have a differential to no effect on behavior (45–47). To test whether MEF2 activity could enhance a cognitive function in a disease context, we first sought to determine whether the subpopulation of excitatory neurons that showed increased expression of MEF2C and MEF2C targets in cognitively resilient humans might exist in the mouse cortex. Using a published dataset of single-cell RNA sequencing from the mouse prefrontal cortex, we identified the cells corresponding to wild-type, control adult mice (24,822 cells) and performed dimensionality reduction and clustering via UMAP analysis (48). As published, we identified all major cell types known in the brain (fig. S10A) and were able to identify excitatory neurons by coexpression of *Snap25* and *Slc17a7* (fig. S10B). We next performed subcluster analysis of the excitatory neurons (14,522 cells) by subsetting these cells and reperforming UMAP analysis to identify six different subclusters of excitatory neurons (fig. S10C). We then assessed for enrichment of the top 50 genes enriched in the Ex2 subcluster within the mouse excitatory neuron subclusters and did not identify any mouse subcluster that appeared to share a homology with Ex2 (fig. S10D).

The absence of a specific mouse subcluster of neurons to target and the translational potential of broad overexpression led us to generate an Adeno-associated virus (AAV)-PHP.eB virus, known to predominantly transduce neurons (enhanced central nervous system transduction from AAV.PHP.eB infusion into the cisterna magna of older adult rats compared to AAV), and a lentivirus to overexpress *Mef2a* and *Mef2c* in addition to *GFP* under the regulation of constitutive cytomegalovirus promoter. Control animals were injected with viral constructs that expressed *GFP* alone. RNA in situ hybridization revealed viral *GFP* expression along with modest but significant up-regulation of *Mef2c* and two target genes, *Scn1a* and *Gria4* (fig. S11A; *Mef2c*, $P < 0.0001$; *Scn1a*, $P = 0.0012$; *Gria4*, $P < 0.0001$). Young (3 months old) wild-type male mice overexpressing *Mef2a/c* displayed enhanced rates of extinction after fear conditioning compared to control animals (fig. S11B; unpaired *t* test comparing % freezing after two shocks and % freezing on the last day of extinction training; *t* test, P value for *GFP* control group = 0.0709; *t* test, P value for *Mef2a/c* OE group = 0.0047) without displaying differences in baseline freezing, locomotion or body weight (fig. S11, C and D),

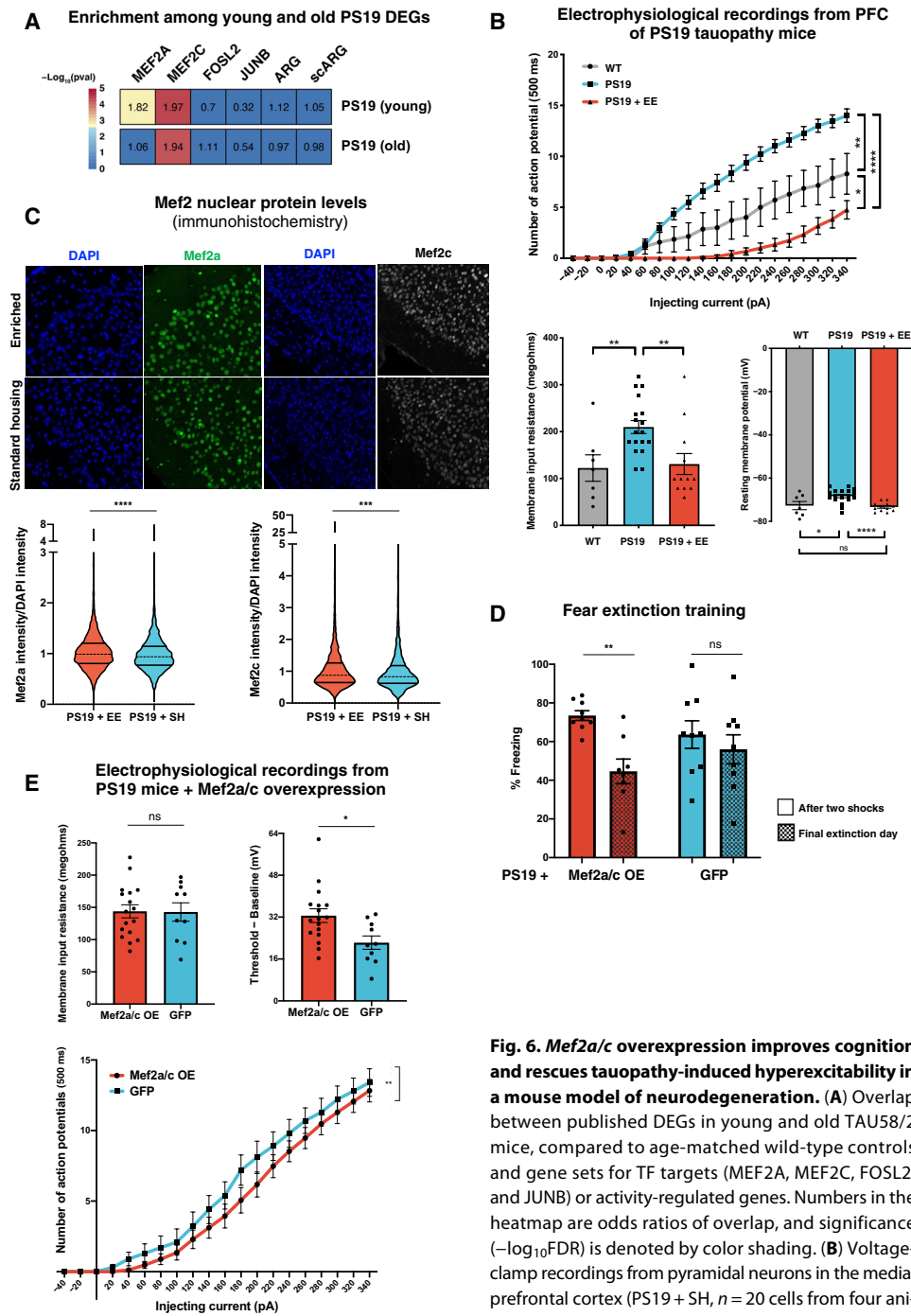


Fig. 6. *Mef2a/c* overexpression improves cognition and rescues tauopathy-induced hyperexcitability in a mouse model of neurodegeneration. (A) Overlap between published DEGs in young and old TAU58/2 mice, compared to age-matched wild-type controls and gene sets for TF targets (MEF2A, MEF2C, FOSL2, and JUNB) or activity-regulated genes. Numbers in the heatmap are odds ratios of overlap, and significance ($-\log_{10}FDR$) is denoted by color shading. (B) Voltage-clamp recordings from pyramidal neurons in the medial prefrontal cortex (PS19 + SH, $n = 20$ cells from four animals; PS19 + EE, $n = 15$ cells from three animals; WT, $n = 9$ cells from two animals) to quantify hyperexcitability as measured by number of action potentials

in 500 ms for a given injecting current (top), membrane resistance (bottom left), and resting membrane potential (bottom right). (C) Top: IHC from the medial prefrontal cortex of PS19 male mice exposed to EE and SH conditions, staining for DAPI (blue), MEF2A (green), and MEF2C (white). Bottom: Imapr quantification of IHC with MEF2A/DAPI and MEF2C/DAPI intensity plotted for individual nuclei across three EE and three SH mice. (D) Fear extinction learning was assessed in 6-month-old male PS19 mice that were treated with *Mef2a/c* or *GFP* overexpressing viral constructs ($n = 9$ mice per group). (E) Top: Voltage-clamp recordings from GFP-positive pyramidal neurons from mice overexpressing either *Mef2a/c* and *GFP* ($n = 17$ cells from three animals) or *GFP* alone ($n = 10$ cells from three animals) to quantify membrane input resistance (top left), the difference between baseline voltage and action potential threshold (top right), and hyperexcitability as measured by number of action potential fired in 500 ms for a given injection current (bottom).

suggesting a general role for the MEF2 family in promoting cognitive flexibility. At 6 months of age, we performed fear extinction training on PS19 mice to determine whether *Mef2a/c* overexpression is sufficient to enhance cognitive function in the absence of enrichment. Whereas there was no difference in body weight or the initial memory acquisition after two-shock fear conditioning, PS19 mice overexpressing *Mef2a/c* showed faster extinction of the fear memory compared to their control littermates (Fig. 6D; unpaired *t* test comparing % freezing after two shocks and % freezing on the last day of extinction training; *t* test, *P* value for *GFP* control group = 0.6207; *t* test, *P* value for *Mef2a/c* OE group = 0.0057), despite showing similar amounts of phosphorylated tau pathological burden (fig. S11E; unpaired *t* test, *P* = 0.11). Last, using the lentiviral construct, which enabled easier ex vivo identification of transfected neurons, we performed electrophysiological recordings from the prefrontal cortex of PS19 mice overexpressing *Mef2a/c* and the GFP control construct. Whereas we did not observe a change in membrane resistance (Fig. 6E, top left), we found a significant increase in the voltage required to achieve action potential firing threshold from baseline in neurons overexpressing *Mef2a/c* compared to control neurons, consistent with a reduced propensity for neuronal hyperexcitability (Fig. 6E, top right; unpaired *t* test, *P* = 0.0143). We also observed a modest but significant reduction in action potential frequency upon current injection (Fig. 6E, bottom; two-way ANOVA, *P* < 0.01 for group). Collectively, these results highlight that promoting activity of the MEF2 transcriptional network, in the absence of enrichment, is sufficient to induce CgR even in the presence of neurodegenerative pathology in mice. Furthermore, the data suggest that a potential mechanism of the benefits afforded by MEF2-mediated CgR could be the buffering of hyperexcitability that is commonly associated with neurodegenerative disease progression and pathology.

DISCUSSION

The molecular mechanisms that endogenously prevent against cognitive decline are largely unknown; if identified,

they have the potential to improve a central facet of human health in our aging population. Our work uncovers a link between MEF2-dependent transcriptional programs and cognitive health throughout life, in which MEF2 activity contributes to enhanced cognitive function at baseline and CgR in the face of neuropathology. We began by studying the molecular changes that arise from the most potent known inducer of CgR, EE. Analysis of global chromatin and transcriptional changes in mouse cortical neurons led to the identification of MEF2 TFs as key modulators of neural function after enrichment. Transcriptional activity of the MEF2 regulatory network is increased upon chronic enrichment, and by knocking down *Mef2a* and *Mef2c*, we show that these TFs are required to actualize the cognitive benefits of an enriched environment.

To broaden the translational relevance of our animal work, we performed experiments in both male and female mice, in different strains of mice, in wild-type and genetic disease models, and in mice of varying ages. We consistently see involvement of the MEF2 network after enrichment, suggesting that this phenomenon is not limited to a particular sex, age, or genetic background and may be more broadly applicable to counteracting disease. Our analysis of human tissue does exhibit a sex bias, which remains a limitation of the study.

The molecular mechanisms mediating CgR in humans have been difficult to define because of a lack of integration between clinical measures and unbiased, comprehensive molecular data. We interrogated phenotypic and bulk brain RNA sequencing data from two large independent databases (ROSMAP and MSBB) and found that increased expression of *MEF2C* and downstream targets were associated with overall cognition and CgR. In addition, we used single-nucleus RNA sequencing and showed that the increase in *MEF2C* expression in cognitively resilient cells occurs in a subset of excitatory neurons that appear to be translationally active. This was particularly intriguing as it suggests that cortical neurons that are actively responding to and encoding environmental stimuli require up-regulation of the MEF2 network in the face of pathology to maintain cognitive function. Additional work must be done to further define this particular subset of excitatory neurons, especially in comparison to our findings in mice, which suggest more broad increases in MEF2 activity after enrichment. The marker genes that define Ex2 do not appear to define any excitatory neuron subcluster from mouse cortical tissue, which could be the result of evolutionary divergence or the presence of considerable neuropathology in both groups of our human cohort. Nonetheless, the observation that broad-scale overexpression of *Mef2a/c* can rescue tauopathy-induced hyperexcitability and is sufficient to enhance fear extinction learning in both wild-type mice and a mouse model of neurodegeneration heightens the translational potential of therapeutic targets aimed at modulating MEF2A/C activity broadly in human adults to promote cognitive flexibility and protection.

Up-regulation of *Mef2a* and *Mef2c* in a mouse model of tauopathy does not affect tau pathology. This suggests that the link between MEF2 and tau pathology is not bidirectional: Whereas tau pathology affects expression of the MEF2 network, changes in *Mef2* expression can have a beneficial effect on neuronal excitability and cognition without affecting tau pathology. This distinction may be influenced by a number of factors, including marked transgene overexpression in the PS19 model. In addition, MEF2 targets are predominantly synaptic and channel genes, not kinases, which have a more direct effect on tau phosphorylation. This finding is particularly notable

because it demonstrates the ability to rescue features of neuronal signaling and cognition without needing to affect underlying protein pathology, thus suggesting that activating the MEF2 network may be therapeutically relevant even in cases where the accumulation of pathology is underway.

An intuitive explanation for the link between EE, MEF2 network activity, and cognitive enhancement is that the benefits of enrichment result from the transcriptional output of increased neuronal activity and that MEF2 TFs are part of this activity-induced network because they have long been implicated in activity-dependent regulation of gene expression in neurons (9). To test this hypothesis, we compared both enrichment DEGs in mice and CgR-associated genes in humans to two datasets capturing transcriptional changes after generic neuronal activity (ARG and scARG) but did not observe meaningful overlap. This finding emphasizes the specificity of MEF2's involvement in enrichment-induced CgR, pointing to a unique type of activity or a specific subset of molecular drivers that are enabled in the context of positive and stimulating experiences to afford a phenotypic benefit. This is not completely unexpected given that several activities that induce heightened neuronal activity, such as drug use or traumatic events, are not associated with the preservation of cognitive health.

Although our primary goal with this work is to prevent cognitive symptoms of neurodegeneration, these findings may be extended to better understand baseline features of human cognition. We examined one aspect of cognitive function often linked to intelligence, the ability to quickly and effectively integrate new information into existing schemas. Manipulating expression of *Mef2* had profound effects on this ability, thereby providing insight into the potential neural mechanisms of cognitive flexibility that extend beyond implications for neurodegenerative disease.

How does MEF2-dependent activity in the prefrontal cortex link EE to CgR? This very likely occurs in a temporally and spatially specific manner because previous work has shown that increasing expression of *Mef2* in the dentate gyrus blocks spatial memory formation, whereas overexpression in the cortex can facilitate learning. Our single-cell results point to a particular subset of neurons within the human cortex being important mediators of MEF2-dependent CgR. The increases in MEF2 TF activity that we observed here likely have a myriad of effects that will need to be further elucidated in subsequent studies, but one critical aspect uncovered here and consistent with the literature is their ability to modulate excitatory: inhibitory (E/I) balance in neural circuits (26, 49). An increase in E/I ratio in the prefrontal cortex has already been linked to a profound impairment in cellular information processing and impairments in conditioned learning (50). Because hyperexcitability has a toxic effect in multiple models of neurodegenerative and neuropsychiatric diseases, a MEF2-induced dampening of the E/I balance could decrease hyperexcitability in a diseased state, thereby explaining how enrichment and MEF2 activity buffer cognitive capacity in the context of neuropathology. MEF2 might also act in a mechanism similar to ARC, helping to establish homeostasis in a highly stimulated brain.

Whereas, in humans, *MEF2C* appears to be more strongly correlated with cognition than *MEF2A*, our mouse work points to a potential role for both *Mef2a* and *Mef2c* in coordinating cognitive function and resilience after enrichment. This discrepancy could have multiple origins and does remain a limitation of the study. First, we could actually be elucidating slightly different processes in mice and

humans. Unfortunately, because of the limitations of human research and the MSBB/ROSMAP databases, we cannot ascertain definitively what led to the induction of increased CgR or the myriad of reasons why end-stage cognition differs across individuals. This could be due to multiple factors, only one of which is differential cognitive stimulation. In our mice work, however, we specifically control the exposure (EE) that induces cognitive enhancement and resilience. As a result, the MEF2 family may govern different facets of ensuring optimal cognitive function and neuronal resilience. Taken in the context of previous work that showed no impact on learning memory with postnatal knockdown of *Mef2c*, it may be that MEF2A and MEF2C activity are conditionally required for actualizing cognitive benefits in the presence of a positive stimulus, such as mental stimulation or EE. Second, there appears to be a divergence in the expression of *Mef2a* between mice and humans. Both our single-cell experiments and analysis of bulk transcriptomic data show a much more modest expression of MEF2A compared to MEF2C in the human cortex. In mice, however, neuronal expression of *Mef2a* and *Mef2c* appear more equal, suggesting that *Mef2a* may have differential roles in mice and human cortical neurons. To this end, the unique presence of MEF2 response elements in higher-order mammals, and their corresponding absence in lower mammals such as mice, has led to the identification of previously unrecognized roles for Mef2 enhancer activity specifically in nonhuman primates (51). The clear involvement of MEF2 in regulating cognition in mice points to a conservation of this particular function in rodents, but further work will be required to further elucidate the individual contribution of *Mef2a* and *Mef2c* to cognitive health, and what aspects of this function may be unique to humans versus conserved across a broader subset of mammalian species.

Overall, the long-standing clinical and epidemiological observation of CgR affords us the potential to better understand how the brain naturally adapts and responds to the presence of pathology. Taking advantage of this powerful phenomenon, this work highlights an important step toward elucidating a set of molecular targets that can guide the development of therapeutics to promote general cognitive health and protect the brain from various forms of neural insult.

MATERIALS AND METHODS

Study design

The goal of this study was to identify a molecular driver of CgR. First, we identified neurotranscriptomic correlates of both enrichment (in mice) and CgR (in humans burdened with neuropathology) in an unbiased manner. Second, we manipulated these TFs in a neurodegenerative disease model and measured properties of neuronal excitability. For all studies, mice were age- and gender-matched to keep treatment and control groups as similar as possible. Enrichment studies lasted 1 month to ensure robustness of the environmental manipulation. For mouse sequencing and immunohistochemistry experiments, all groups were processed and stained at the same time. Imaging quantification was carried out in a blinded fashion by a researcher who did not perform the immunohistochemistry. For human sequencing experiments, samples were processed in batches that spanned both resilient and nonresilient individuals in case of batch effects. Inclusion criteria for cognitively resilient and nonresilient individuals were based on the neuropathological and cognitive spread of the ROS/MAP cohort, with care to match groups on other clinical

metrics and demographic data. We excluded outliers in the human snRNA sequencing experiment based on overall sequencing quality and cell clustering.

Statistics

Molecular results are presented as means \pm SEM, assuming a normal distribution. All nonsequencing statistical analyses used Prism GraphPad software to compute significance. Data limited to two experimental groups were analyzed by two-tailed unpaired *t* tests. Data consisting of three or more groups were analyzed by one- or two-way ANOVAs followed by pairwise multiple comparisons tests. The statistical test, *P* values, and sample size (*n*) for each experiment are specified in the figure legends. No statistical method was used to estimate sample size, but they are consistent with previous publications while attempting to eliminate waste and animal mortality. Molecular analyses used a minimum of three biological replicates per condition, and validation experiments used a distinct set of animals. Behavioral tests were run on at least two independent cohorts of animals, with one reported in the main figures.

SUPPLEMENTARY MATERIALS

www.science.org/doi/10.1126/scitranslmed.abd7695

Supplementary Methods

Figs. S1 to S11

Tables S1 to S13

Data file S1

References (52–61)

[View/request a protocol for this paper from Bio-protocol.](#)

REFERENCES AND NOTES

1. S. H. Woolf, H. Schoemaker, Life expectancy and mortality rates in the United States, 1959–2017. *JAMA* **322**, 1996–2016 (2019).
2. G. C. Brown, Living too long. *EMBO Rep.* **16**, 137–141 (2015).
3. Y. Stern, B. Gurland, T. K. Tatemichi, M. X. Tang, D. Wilder, R. Mayeux, Influence of education and occupation on the incidence of Alzheimer's disease. *JAMA* **271**, 1004–1010 (1994).
4. A. van Dellen, C. Blakemore, R. Deacon, D. York, A. J. Hannan, Delaying the onset of Huntington's in mice. *Nature* **404**, 721–722 (2000).
5. J. L. Jankowsky, Environmental enrichment mitigates cognitive deficits in a mouse model of Alzheimer's disease. *J. Neurosci.* **25**, 5217–5224 (2005).
6. M. Solinas, C. Chauvet, N. Thiriet, R. El Rawas, M. Jaber, Reversal of cocaine addiction by environmental enrichment. *Proc. Natl. Acad. Sci. U.S.A.* **105**, 17145–17150 (2008).
7. M. L. Lehmann, M. Herkenham, Environmental enrichment confers stress resiliency to social defeat through an infralimbic cortex-dependent neuroanatomical pathway. *J. Neurosci.* **31**, 6159–6173 (2011).
8. J. Leon, A. J. Moreno, B. I. Garay, R. J. Chalkley, A. L. Burlingame, D. Wang, D. B. Dubal, Peripheral elevation of a klotho fragment enhances brain function and resilience in young, aging, and α -synuclein transgenic mice. *Cell Rep.* **20**, 1360–1371 (2017).
9. S. W. Flavell, C. W. Cowan, T.-K. Kim, P. L. Greer, Y. Lin, S. Paradis, E. C. Griffith, L. S. Hu, C. Chen, M. E. Greenberg, Activity-dependent regulation of MEF2 transcription factors suppresses excitatory synapse number. *Science* **311**, 1008–1012 (2006).
10. S. Pulipparacharuvil, W. Renthall, C. F. Hale, M. Taniguchi, G. Xiao, A. Kumar, S. J. Russo, D. Sikder, C. M. Dewey, M. M. Davis, P. Greengard, A. C. Nairn, E. J. Nestler, C. W. Cowan, Cocaine regulates MEF2 to control synaptic and behavioral plasticity. *Neuron* **59**, 621–633 (2008).
11. B. Gaudilliere, Y. Shi, A. Bonni, RNA interference reveals a requirement for myocyte enhancer factor 2A in activity-dependent neuronal survival. *J. Biol. Chem.* **277**, 46442–46446 (2002).
12. S. Sniekers, S. Stringer, K. Watanabe, P. R. Jansen, J. R. I. Coleman, E. Krapohl, E. Taskesen, A. R. Hammerschlag, A. Okbay, D. Zabaneh, N. Amin, G. Breen, D. Cesarini, C. F. Chabris, W. G. Iacono, M. A. Ikram, M. Johannesson, P. Koellinger, J. J. Lee, P. K. E. Magnusson, M. McGue, M. B. Miller, W. E. R. Ollier, A. Payton, N. Pendleton, R. Plomin, C. A. Rietveld, H. Tiemeier, C. M. van Duijn, D. Posthuma, Genome-wide association meta-analysis of 78,308 individuals identifies new loci and genes influencing human intelligence. *Nat. Genet.* **49**, 1107–1112 (2017).

13. D. A. Bennett, J. A. Schneider, Z. Arvanitakis, R. S. Wilson, Overview and findings from the religious orders study. *Curr. Alzheimer Res.* **9**, 628–645 (2012).
14. D. A. Bennett, J. A. Schneider, A. S. Buchman, L. L. Barnes, P. A. Boyle, R. S. Wilson, Overview and findings from the rush Memory and Aging Project. *Curr. Alzheimer Res.* **9**, 646–663 (2012).
15. A. Zeleznikow-Johnston, E. L. Burrows, T. Renoir, A. J. Hannan, Environmental enrichment enhances cognitive flexibility in C57BL/6 mice on a touchscreen reversal learning task. *Neuropharmacology* **117**, 219–226 (2017).
16. I. Lahiani-Cohen, A. Loubopoulos, E. Haber, L. Rozenstein-Tsakovich, O. Abramsky, N. Grigoriadis, H. Rosenmann, Moderate environmental enrichment mitigates tauopathy in a neurofibrillary tangle mouse model. *J. Neuropathol. Exp. Neurol.* **70**, 610–621 (2011).
17. G. Lach, M. A. Bicca, A. A. Hoeller, E. C. D. S. Santos, A. P. R. Costa, T. C. M. de Lima, Short-term enriched environment exposure facilitates fear extinction in adult rats: The NPY-Y1 receptor modulation. *Neuropeptides* **55**, 73–78 (2016).
18. A. Fischer, F. Sananbenesi, X. Wang, M. Dobbin, L.-H. Tsai, Recovery of learning and memory is associated with chromatin remodelling. *Nature* **447**, 178–182 (2007).
19. J. D. Buenostro, P. G. Giresi, L. C. Zaba, H. Y. Chang, W. J. Greenleaf, Transposition of native chromatin for fast and sensitive epigenomic profiling of open chromatin, DNA-binding proteins and nucleosome position. *Nat. Methods* **10**, 1213–1218 (2013).
20. R. Halder, M. Hennion, R. O. Vidal, O. Shomroni, R.-U. Rahman, A. Rajput, T. P. Centeno, F. van Bebber, V. Capece, J. C. G. Vizzaino, A.-L. Schuetz, S. Burkhardt, E. Benito, M. N. Sala, S. B. Javan, C. Haass, B. Schmid, A. Fischer, S. Bonn, DNA methylation changes in plasticity genes accompany the formation and maintenance of memory. *Nat. Neurosci.* **19**, 102–110 (2016).
21. S. Wales, S. Hashemi, A. Blais, J. C. McDermott, Global MEF2 target gene analysis in cardiac and skeletal muscle reveals novel regulation of DUSP6 by p38MAPK-MEF2 signaling. *Nucleic Acids Res.* **42**, 11349–11362 (2014).
22. X. Zhang, J. Y. Jin, J. Wu, X. Qin, R. Streilein, R. P. Hall, J. Y. Zhang, RNA-seq and ChIP-seq reveal SQSTM1/p62 as a key mediator of JunB suppression of NF- κ B-dependent inflammation. *J. Invest. Dermatol.* **135**, 1016–1024 (2015).
23. J. S. Davies, D. C. Klein, D. A. Carter, Selective genomic targeting by FRA-2/FOSL2 transcription factor: Regulation of the Rgs4 gene is mediated by a variant activator protein 1 (AP-1) promoter sequence/CREB-binding protein (CBP) mechanism. *J. Biol. Chem.* **286**, 15227–15239 (2011).
24. S. P. Majidi, N. C. Reddy, M. J. Moore, H. Chen, T. Yamada, M. M. Andzelm, T. J. Cherry, L. S. Hu, M. E. Greenberg, A. Bonni, Chromatin environment and cellular context specify compensatory activity of paralogous MEF2 transcription factors. *Cell Rep.* **29**, 2001–2015.e5 (2019).
25. F. Telese, Q. Ma, P. M. Perez, D. Notani, S. Oh, W. Li, D. Comoletti, K. A. Ohgi, H. Taylor, M. G. Rosenfeld, LRP8-reeelin-regulated neuronal enhancer signature underlying learning and memory formation. *Neuron* **86**, 696–710 (2015).
26. A. J. Harrington, A. Raisi, K. Rajkovich, S. Berto, J. Kumar, G. Molinaro, J. Raduazzo, Y. Guo, K. Loerwald, G. Konopka, K. M. Huber, C. W. Cowan, MEF2C regulates cortical inhibitory and excitatory synapses and behaviors relevant to neurodevelopmental disorders. *eLife* **5**, e20059 (2016).
27. B. Lacar, S. B. Linker, B. N. Jaeger, S. Krishnaswami, J. Barron, M. Kelder, S. Parylak, A. A. Paquola, P. Venepally, M. Novotny, C. O. A. Connor, C. Fitzpatrick, J. Erwin, J. Y. Hsu, D. Husband, M. J. McConnell, R. Lasken, F. H. Gage, Nuclear RNA-seq of single neurons reveals molecular signatures of activation. *Nat. Commun.* **7**, 11022 (2016).
28. K. M. Tyssowski, N. R. DeStefino, J.-H. Cho, C. J. Dunn, R. G. Poston, C. E. Carty, R. D. Jones, S. M. Chang, P. Romeo, M. K. Wurzelmann, J. M. Ward, M. L. Andermann, R. N. Saha, S. M. Dudek, J. M. Gray, Different neuronal activity patterns induce different gene expression programs. *Neuron* **98**, 530–546.e11 (2018).
29. K. M. Frick, N. A. Stearns, J.-Y. Pan, J. Berger-Sweeney, Effects of environmental enrichment on spatial memory and neurochemistry in middle-aged mice. *Learn. Mem.* **10**, 187–198 (2003).
30. J. Krell-Roesch, P. Vemuri, A. Pink, R. O. Roberts, G. B. Stokin, M. M. Mielke, T. J. H. Christianson, D. S. Knopman, R. C. Petersen, W. K. Kremers, Y. E. Geda, Association between mentally stimulating activities in late life and the outcome of incident mild cognitive impairment, with an analysis of the APOE ϵ 4 genotype. *JAMA Neurol.* **74**, 332–338 (2017).
31. Q. Ma, F. Telese, Genome-wide epigenetic analysis of MEF2A and MEF2C transcription factors in mouse cortical neurons. *Commun. Integr. Biol.* **8**, e1087624 (2015).
32. K. E. Rajkovich, K. W. Loerwald, C. F. Hale, C. T. Hess, J. R. Gibson, K. M. Huber, Experience-dependent and differential regulation of local and long-range excitatory neocortical circuits by postsynaptic Mef2c. *Neuron* **93**, 48–56 (2017).
33. D. J. Selkoe, Early network dysfunction in Alzheimer's disease. *Science* **365**, 540–541 (2019).
34. J. Wang, S.-W. Ou, Y.-J. Wang, Distribution and function of voltage-gated sodium channels in the nervous system. *Channels* **11**, 534–554 (2017).
35. A. Escayg, B. T. MacDonald, M. H. Meisler, S. Baulac, G. Huberfeld, I. An-Gourfinkel, A. Brice, E. LeGuern, B. Moulard, D. Chaigne, C. Buresi, A. Malafosse, Mutations of SCN1A, encoding a neuronal sodium channel, in two families with GEF5+2. *Nat. Genet.* **24**, 343–345 (2000).
36. Y. Ohno, S. Ishihara, T. Mashimo, N. Sofue, S. Shimizu, T. Imaoku, T. Tsurumi, M. Sasa, T. Serikawa, Scn1a missense mutation causes limbic hyperexcitability and vulnerability to experimental febrile seizures. *Neurobiol. Dis.* **41**, 261–269 (2011).
37. B. Beyer, C. Deleuze, V. A. Letts, C. L. Mahaffey, R. M. Boumil, T. A. Lew, J. R. Huguenard, W. N. Frankel, Absence seizures in C3H/HeJ and knockout mice caused by mutation of the AMPA receptor subunit Gria4. *Hum. Mol. Genet.* **17**, 1738–1749 (2008).
38. C. L. Stopford, J. C. Thompson, D. Neary, A. M. T. Richardson, J. S. Snowden, Working memory, attention, and executive function in Alzheimer's disease and frontotemporal dementia. *Cortex* **48**, 429–446 (2012).
39. E. Y. Chen, C. M. Tan, Y. Kou, Q. Duan, Z. Wang, G. V. Meirelles, N. R. Clark, A. Ma'ayan, Enrich: Interactive and collaborative HTML5 gene list enrichment analysis tool. *BMC Bioinformatics* **14**, 128 (2013).
40. J. A. Miller, S.-L. Ding, S. M. Sunkin, K. A. Smith, L. Ng, A. Szafer, A. Ebbert, Z. L. Riley, J. J. Royall, K. Aiona, J. M. Arnold, C. Bennet, D. Bertagnolli, K. Brouner, S. Butler, S. Caldejon, A. Carey, C. Cuhacyan, R. A. Dalley, N. Dee, T. A. Dolbear, B. A. C. Facer, D. Feng, T. P. Fliss, G. Gee, J. Goldy, L. Gourley, B. W. Gregor, G. Gu, R. E. Howard, J. M. Jochim, C. L. Kuan, C. Lau, C.-K. Lee, F. Lee, T. A. Lemon, P. Lesnar, B. McMurray, N. Mastan, N. Mosqueda, T. Nalwai-Cecchini, N.-K. Ngo, J. Nyhus, A. Oldre, E. Olson, J. Parente, P. D. Parker, S. E. Parry, A. Stevens, M. Pletikos, M. Reding, K. Roll, D. Sandman, M. Sarreal, S. Shapouri, N. V. Shapovalova, E. H. Shen, N. Sjoquist, C. R. Slaughterbeck, M. Smith, A. J. Sodt, D. Williams, L. Zöllei, B. Fischl, M. B. Gerstein, D. H. Geschwind, I. A. Glass, M. J. Hawrylycz, R. F. Hevner, H. Huang, A. R. Jones, J. A. Knowles, P. Levitt, J. W. Phillips, N. Šestan, P. W. Wohnoutka, C. Dang, A. Bernard, J. G. Hohmann, E. S. Lein, Transcriptional landscape of the prenatal human brain. *Nature* **508**, 199–206 (2014).
41. Z. He, D. Han, O. Efimova, P. Guijarro, Q. Yu, A. Oleksiak, S. Jiang, K. Anokhin, B. Velichkovsky, S. Grünwald, P. Khaitovich, Comprehensive transcriptome analysis of neocortical layers in humans, chimpanzees and macaques. *Nat. Neurosci.* **20**, 886–895 (2017).
42. Y. Yoshiyama, M. Higuchi, B. Zhang, S.-M. Huang, N. Iwata, T. C. Saïdo, J. Maeda, T. Suhara, J. Q. Trojanowski, V. M. Y. Lee, Synapse loss and microglial activation precede tangles in a P301S tauopathy mouse model. *Neuron* **53**, 337–351 (2007).
43. Y. D. Ke, G. Chan, K. Stefanoska, C. Au, M. Bi, B. J. Müller, M. Przybyla, A. Feiten, E. Prikas, G. M. Halliday, O. Piguet, M. C. Kiernan, M. C. Kassio, J. R. Hodges, C. T. Loy, J. S. Mattick, A. Ittner, J. J. Kril, G. T. Sutherland, L. M. Ittner, CNS cell type-specific gene profiling of P301S tau transgenic mice identifies genes dysregulated by progressive tau accumulation. *J. Biol. Chem.* **294**, 14149–14162 (2019).
44. S. Maeda, B. Djukic, P. Taneja, G.-Q. Yu, I. Lo, A. Davis, R. Craft, W. Guo, X. Wang, D. Kim, R. Ponnusamy, T. M. Gill, E. Masliah, L. Mucke, Expression of A152T human tau causes age-dependent neuronal dysfunction and loss in transgenic mice. *EMBO Rep.* **17**, 530–551 (2016).
45. A. C. Mitchell, B. Javidfar, V. Pothula, D. Ibi, E. Y. Shen, C. J. Peter, L. K. Bicks, T. Fehr, Y. Jiang, K. J. Brennand, R. L. Neve, J. Gonzalez-Maeso, S. Akbarian, MEF2C transcription factor is associated with the genetic and epigenetic risk architecture of schizophrenia and improves cognition in mice. *Mol. Psychiatry* **23**, 123–132 (2018).
46. C. J. Cole, V. Mercaldo, L. Restivo, A. P. Yiu, M. J. J. Kerkes, J.-H. Han, G. Vetere, T. Pekar, P. J. Ross, R. L. Neve, P. W. Frankland, S. A. Josselyn, MEF2 negatively regulates learning-induced structural plasticity and memory formation. *Nat. Neurosci.* **15**, 1255–1264 (2012).
47. M. Adachi, P.-Y. Lin, H. Pranav, L. M. Monteggia, Postnatal loss of Mef2c results in dissociation of effects on synapse number and learning and memory. *Biol. Psychiatry* **80**, 140–148 (2016).
48. A. Bhattacharjee, M. N. Djekidel, R. Chen, W. Chen, L. M. Tuesta, Y. Zhang, Cell type-specific transcriptional programs in mouse prefrontal cortex during adolescence and addiction. *Nat. Commun.* **10**, 4169 (2019).
49. S. Tu, M. W. Akhtar, R. M. Escorihuela, A. Amador-Arjona, V. Swarup, J. Parker, J. D. Zaremba, T. Holland, N. Bansal, D. R. Holohan, K. Lopez, S. D. Ryan, S. F. Chan, L. Yan, X. Zhang, X. Huang, A. Sultan, S. R. McKeercher, R. Ambasadhan, H. Xu, Y. Wang, D. H. Geschwind, A. J. Roberts, A. V. Tersikh, R. A. Rissman, E. Masliah, S. A. Lipton, N. Nakanishi, NitroSynapsin therapy for a mouse MEF2C haploinsufficiency model of human autism. *Nat. Commun.* **8**, 1488 (2017).
50. O. Yizhar, L. E. Fenno, M. Prigge, F. Schneider, T. J. Davidson, D. J. O'Shea, V. S. Sohal, I. Goshen, J. Finkelstein, J. T. Paz, K. Stehfest, R. Fudim, C. Ramakrishnan, J. R. Huguenard, P. Hegemann, K. Deisseroth, Neocortical excitation/inhibition balance in information processing and social dysfunction. *Nature* **477**, 171–178 (2011).
51. B. Ataman, G. L. Boulting, D. A. Harmin, M. G. Yang, M. Baker-Salisbury, E.-L. Yap, A. N. Malik, K. Mei, A. A. Rubin, I. Spiegel, E. Durrezi, N. Sharma, L. S. Hu, M. Pletikos, E. C. Griffith, J. N. Partlow, C. R. Stevens, M. Adli, M. Chahrouh, N. Šestan, C. A. Walsh,

- V. K. Berezovskii, M. S. Livingstone, M. E. Greenberg, Evolution of Osteocrin as an activity-regulated factor in the primate brain. *Nature* **539**, 242–247 (2016).
52. X. Chen, Y. Shen, W. Draper, J. D. Buenrostro, U. Litzenburger, S. W. Cho, A. T. Satpathy, A. C. Carter, R. P. Ghosh, A. East-Seletsky, J. A. Doudna, W. J. Greenleaf, J. T. Liphardt, H. Y. Chang, ATAC-seq reveals the accessible genome by transposase-mediated imaging and sequencing. *Nat. Methods* **13**, 1013–1020 (2016).
53. J. M. Gaspar, Improved peak-calling with MACS2. *bioRxiv* **2018**, 496521 (2018).
54. G. Yu, L.-G. Wang, Q.-Y. He, ChIPseeker: An R/Bioconductor package for ChIP peak annotation, comparison and visualization. *Bioinformatics* **31**, 2382–2383 (2015).
55. Z. Gu, R. Eils, M. Schlesner, N. Ishaque, EnrichedHeatmap: An R/Bioconductor package for comprehensive visualization of genomic signal associations. *BMC Genomics* **19**, 234 (2018).
56. M. D. Robinson, D. J. McCarthy, G. K. Smyth, edgeR: A bioconductor package for differential expression analysis of digital gene expression data. *Bioinformatics* **26**, 139–140 (2010).
57. S. P. Majidi, N. C. Reddy, M. J. Moore, H. Chen, T. Yamada, M. M. Andzelm, T. J. Cherry, L. S. Hu, M. E. Greenberg, A. Bonni, Chromatin environment and cellular context specify compensatory activity of paralogous MEF2 transcription factors. *Cell Rep.* **29**, 2001–2015.e5 (2019).
58. M. Wang, N. D. Beckmann, P. Roussos, E. Wang, X. Zhou, Q. Wang, C. Ming, R. Neff, W. Ma, J. F. Fullard, M. E. Hauberg, J. Bendl, M. A. Peters, B. Logsdon, P. Wang, M. Mahajan, L. M. Mangravite, E. B. Dammer, D. M. Duong, J. J. Lah, N. T. Seyfried, A. I. Levey, J. D. Buxbaum, M. Ehrlich, S. Gandy, P. Katsel, V. Haroutunian, E. Schadt, B. Zhang, The Mount Sinai cohort of large-scale genomic, transcriptomic and proteomic data in Alzheimer's disease. *Sci. Data* **5**, 180185 (2018).
59. N. N. Parikhshak, R. Luo, A. Zhang, H. Won, J. K. Lowe, V. Chandran, S. Horvath, D. H. Geschwind, Integrative functional genomic analyses implicate specific molecular pathways and circuits in autism. *Cell* **155**, 1008–1021 (2013).
60. P. L. de Jager, Y. Ma, C. McCabe, J. Xu, B. N. Vardarajan, D. Felsky, H.-U. Klein, C. C. White, M. A. Peters, B. Logsdon, P. Nejad, A. Tang, L. M. Mangravite, L. Yu, C. Gaiteri, S. Mostafavi, J. A. Schneider, D. A. Bennett, A multi-omic atlas of the human frontal cortex for aging and Alzheimer's disease research. *Sci. Data* **5**, 180142 (2018).
61. H. Mathys, J. Davila-Velderrain, Z. Peng, F. Gao, S. Mohammadi, J. Z. Young, M. Menon, L. He, F. Abdurrob, X. Jiang, A. J. Martorell, R. M. Ransohoff, B. P. Hafler, D. A. Bennett, M. Kellis, L.-H. Tsai, Single-cell transcriptomic analysis of Alzheimer's disease. *Nature* **570**, 332–337 (2019).

Acknowledgments: We would like to thank E. Lockshin, D. von Maydell, P. Narayan, J. Penney, W.-C. Huang, J. Blanche, H. Meharena, A. Marco, and M. Victor who helped edit this work.

Funding: This work was funded by Glenn for Biology of Aging Research #6935778, NIH 1-R01-AG046174-03, NIH RF1-AG054321, and 1-RF1-AG054012 to L.-H.T.; NIH 7-R01-AG058002 to M.K.; Cure Alzheimer's Fund to L.-H.T. and M.K.; P30AG10161, R01AG15819, R01AG17917, and U01AG61356 to D.A.B.; and NICHD T32HD098061 to R.M.R. **Author contributions:** This study was directed by L.-H.T. and designed by S.J.B., R.M.R., and L.-H.T. S.J.B., R.M.R., F.G.-R., K.A., and C.C.P. performed molecular and mouse experiments. J.W. performed all electrophysiology experiments. S.J.B., F.G.-R., F.A., C.C.P., P.L.B., and N.E.P.M. performed imaging analyses and quantification. R.M.R., J.D.-V., and F.G.-R. performed the bioinformatics analyses with guidance from M.K. D.A.B. provided human brain samples and helped with statistical analysis of the ROSMAP data. S.J.B. and R.M.R. wrote the manuscript with major edits from M.K. and L.-H.T. **Competing interests:** D.A.B. serves on the scientific advisory boards of AbbVie, Takeda, Origent Inc., and Vigor Minds. M.K. serves on the scientific advisory boards of the NSF-Simons Center for Multiscale Cell Fate Research (CMCF). L.-H.T. serves on the scientific advisory boards of Cognito Therapeutics, Souvien Therapeutics, Cell Signaling Technology, Yumanity Therapeutics, Metro Bio LLC, and Jupiter Neurosciences Inc. All other authors declare that they have no competing interests. **Data and materials availability:** The MSBB clinical and bulk sequencing data can be accessed via the Synapse portal (Synapse ID: syn3159438). The ROSMAP metadata can be accessed via the Synapse portal (Synapse ID: syn3219045). The data are available under controlled use conditions set by human privacy regulations. To access the data, a data use agreement is needed. This registration is in place solely to ensure anonymity of the ROSMAP study participants. A data use agreement can be agreed with either Rush University Medical Center (RUMC) or with SAGE, who maintains Synapse, and can be downloaded from their websites. The snRNA-seq and bulk sequencing data will be available on The Rush Alzheimer's Disease Center (RADC) Research Resource Sharing Hub at www.radc.rush.edu/docs/omics.htm or via the Synapse portal. The mouse RNA- and ATAC-sequencing data are publicly available (GEO series: GSE176435). All other published datasets used within the study are referenced in the appropriate places within the manuscript text. Code used throughout this study is freely accessible on GitHub (<https://github.com/ravikiran-raju/Mef2>).

Submitted 14 July 2020

Resubmitted 9 June 2021

Accepted 4 October 2021

Published 3 November 2021

10.1126/scitranslmed.abb7695

MEF2 is a key regulator of cognitive potential and confers resilience to neurodegeneration

Scarlett J. Barker, Ravikiran M. Raju, Noah E.P. Milman, Jun Wang, Jose Davila-Velderrain, Fatima Gunter-Rahman, Cameron C. Parro, P. Lorenzo Bozzelli, Fatema Abdurrobkarim Abdelaal, David A. Bennett, Manolis Kellis, Li-Huei Tsai

Sci. Transl. Med., 13 (618), eabd7695. • DOI: 10.1126/scitranslmed.abd7695

Preserving cognition

Neurodegenerative diseases are associated with cognitive impairments. However, few patients are resilient and preserve normal cognition. The mechanisms mediating this phenotype are unclear. Now, Barker *et al.*, using human data and experimental models, report that the expression of the transcription factor MEF2 was a predictor of end-stage cognition in individuals with Alzheimer's disease, and *MEF2* expression was increased in resilient patients. In mice, enriched environment-associated cognitive improvement increased MEF2 activity, whereas *Mef2* KO resulted in cognitive impairments and neuronal overexcitability. Overexpressing *Mef2a/c* in a mouse model of tauopathy improved cognition and reduced overexcitability. The results suggest that MEF2 might be a valuable target for limiting cognitive impairments in patients with neurodegenerative diseases.

View the article online

<https://www.science.org/doi/10.1126/scitranslmed.abd7695>

Permissions

<https://www.science.org/help/reprints-and-permissions>

Use of this article is subject to the [Terms of service](#)